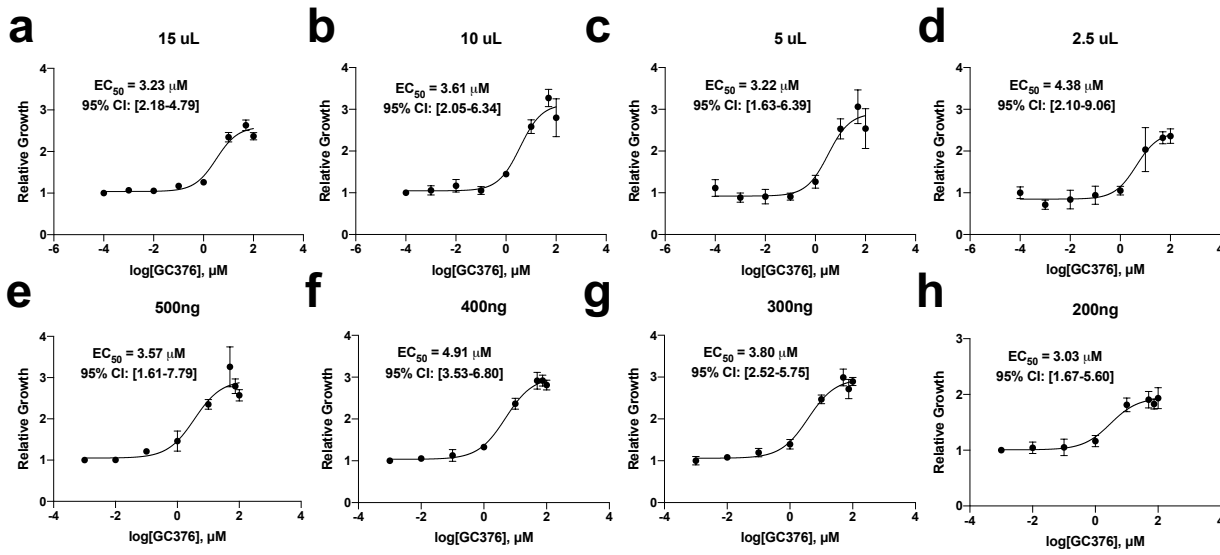


1 Inhibitors of coronavirus 3CL proteases protect cells from protease-mediated cytotoxicity

2 **Supplementary Materials**

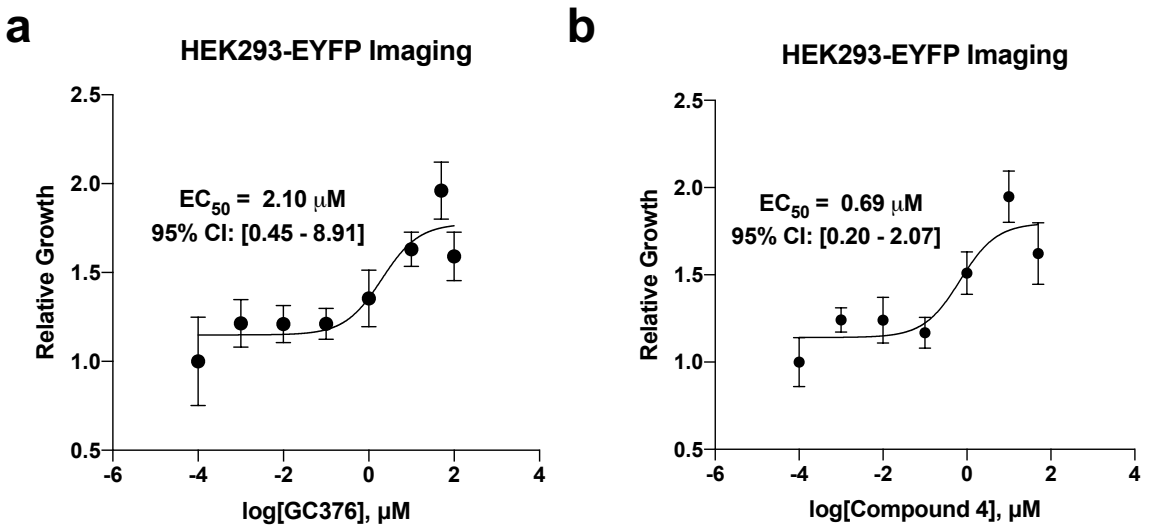
3 **Supplementary Fig. 1. Dose response experiments with SARS-CoV-2 3CLpro and GC376 are robust**
4 **to variable assay parameters.** **a-d.** Repetition of assay with variable levels of cell seeding into drug
5 conditions result in similar EC₅₀ value predictions. **e-h.** Repetition of assay with variable levels of plasmid
6 transfection results in similar EC₅₀ value predictions. EC₅₀ values are displayed as best-fit value alongside
7 95% confidence interval. Data are shown as mean ± s.d. for four technical replicates.



8

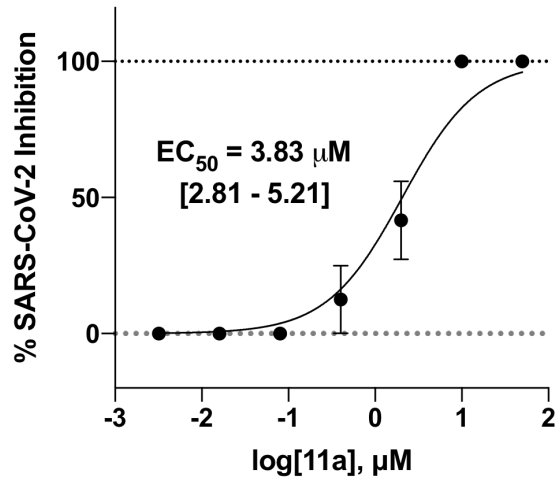
9

10 **Supplementary Fig. 2. Dose response experiments with SARS-CoV-2 3CLpro can be determined with**
11 **imaging of EYFP labeled HEK293 cells.** **a-b.** The activity of GC376 and compound 4 can be detected
12 using imaging rather than crystal violet staining. EC₅₀ values are displayed as best-fit value alongside 95%
13 confidence interval. Data are shown as mean \pm s.d. for four technical replicates.



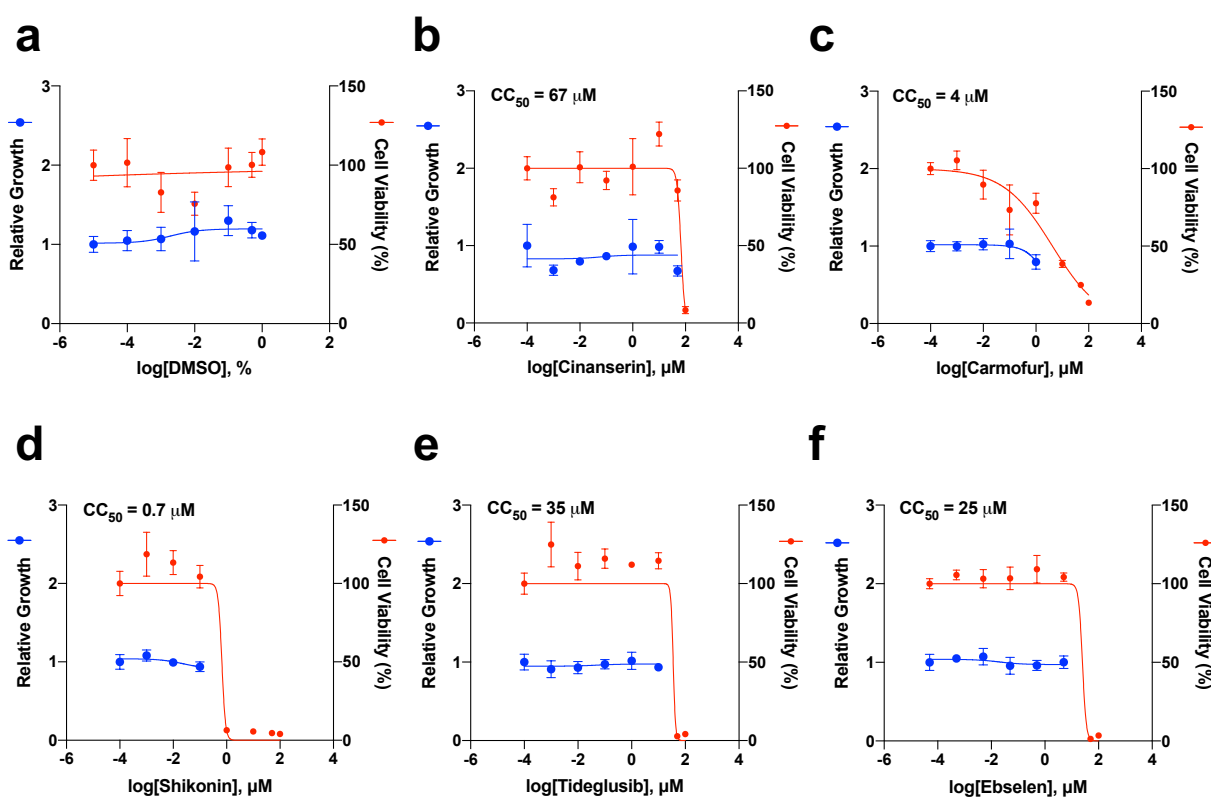
14
15

16 **Supplementary Fig. 3. Live virus testing of 11a.** Live virus testing of 11a against SARS-CoV-2. EC₅₀
17 values are displayed as best-fit value alongside 95% confidence interval. The live virus assay makes use of
18 viral cytopathic effect and was conducted with two biological replicates, each with three technical replicates
19 and the EC₅₀ value was derived from all replicates.



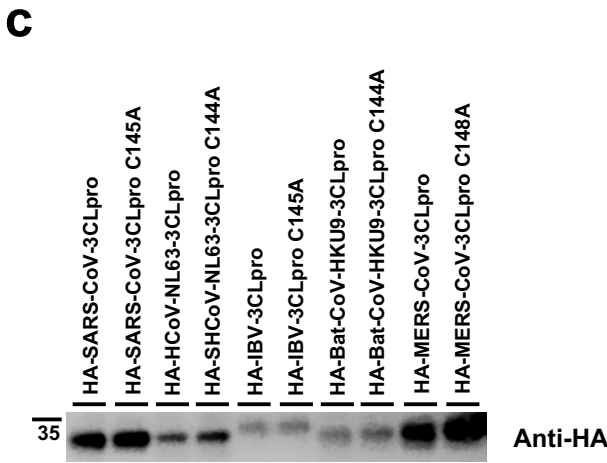
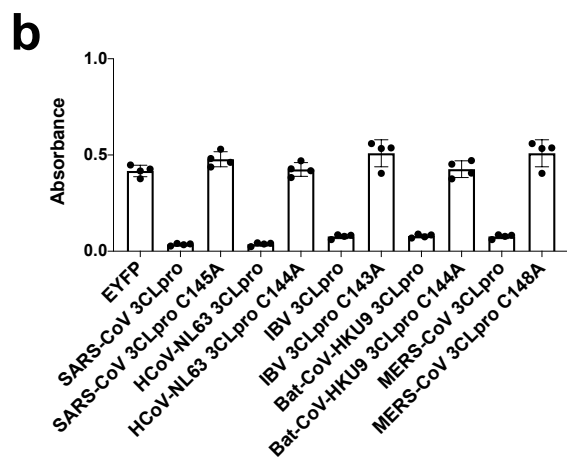
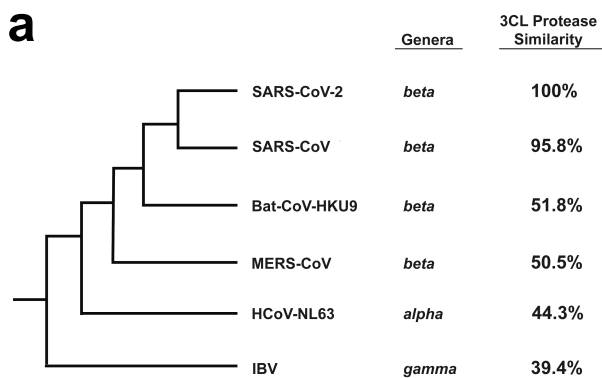
20

21 **Supplementary Fig. 4. Compounds with activity against the SARS-CoV-2 3CLpro *in vitro* that are not**
 22 **efficacious against the SARS-CoV-2 live virus do not show activity in the transfection-based assay.**
 23 a. DMSO was tested at concentrations up to 1%, the maximal concentration used to deliver compounds in
 24 this study, and does not show toxicity to HEK293T cells or protease inhibitory activity against the 3CLpro. b-
 25 e. Other compounds with reported activity against purified SARS-CoV-2 3CLpro but not against live virus. f.
 26 Ebselen, a compound with efficacy against the SARS-CoV-2 live virus does not rescue 3CLpro induced
 27 cytotoxicity within the transfection-based assay. EC₅₀ values are displayed as best-fit value alongside 95%
 28 confidence interval. CC₅₀ values are displayed as best-fit value. Data are shown as mean \pm s.d. for three or
 29 four technical replicates.



30
 31

32 **Supplementary Fig. 5. A number of other 3CLpro enzymes from different coronavirus species also**
 33 **show activity-dependent cytotoxicity.** **a.** A phylogenetic tree of the first six coronaviruses tested in this
 34 study, generated using NCBI Virus with the sequences of the ORF1ab polyprotein. The genera of each virus
 35 are shown along with the amino acid sequence similarity to the SARS-CoV-2 3CLpro calculated using the
 36 default settings on the Protein BLAST tool from NCBI. **b.** Quantification of cytotoxicity upon expression of
 37 active or inactivated 3CLpro enzymes from SARS-CoV, MERS-CoV, Bat-CoV-HKU9, HCoV-NL63, and IBV
 38 in 293T cells. **c.** Western blot detection of HA tagged 3CL proteases. Data are shown as mean \pm s.d. for four
 39 technical replicates.



41 **Supplementary Fig. 6. Variable size, shape, and amino acid composition of 3CL protease S2 pockets.**

42 a. Protein multiple sequence alignments of coronavirus 3CLpros. The sequence alignment was based on

43 chain A of 3CL crystal structures using SARS-CoV-2 as reference. The sequences corresponding to the

44 structural differences near the S2 pocket in the active site were colored. '*' Indicates the varied amino acids

45 which possibly affect the binding of ligands. b. Sequence overlay highlighting structural variability of the S2

46 pocket shown in a red box. Individual structures of 3CLpros demonstrating variable amino acids that can

47 impact compound binding. The S2 pocket of SARS-CoV-2 3CLpro and SARS-CoV 3CLpro are comprised of

48 relatively nonpolar and flexible amino acids. IBV 3CLpro contains an S2 pocket that is smaller in size and is

49 accompanied by a positively charged lysine residue, which may negatively impact the binding of the larger

50 hydrophobic P2 substituents. Additionally, Lys45 of IBV 3CLpro forms a salt bridge with Glu187 in the

51 inhibitor bound crystal structure. The charge interaction may render the S2 pocket of IBV 3CLpro more rigid

52 than SARS-CoV or SARS-CoV-2. MERS-CoV 3CLpro and HCoV-NL63 3CLpro appear to have smaller S2

53 pockets, which unlike SARS-CoV-2 3CLpro and SARS-CoV 3CLpro, is supported by a rigid proline residue

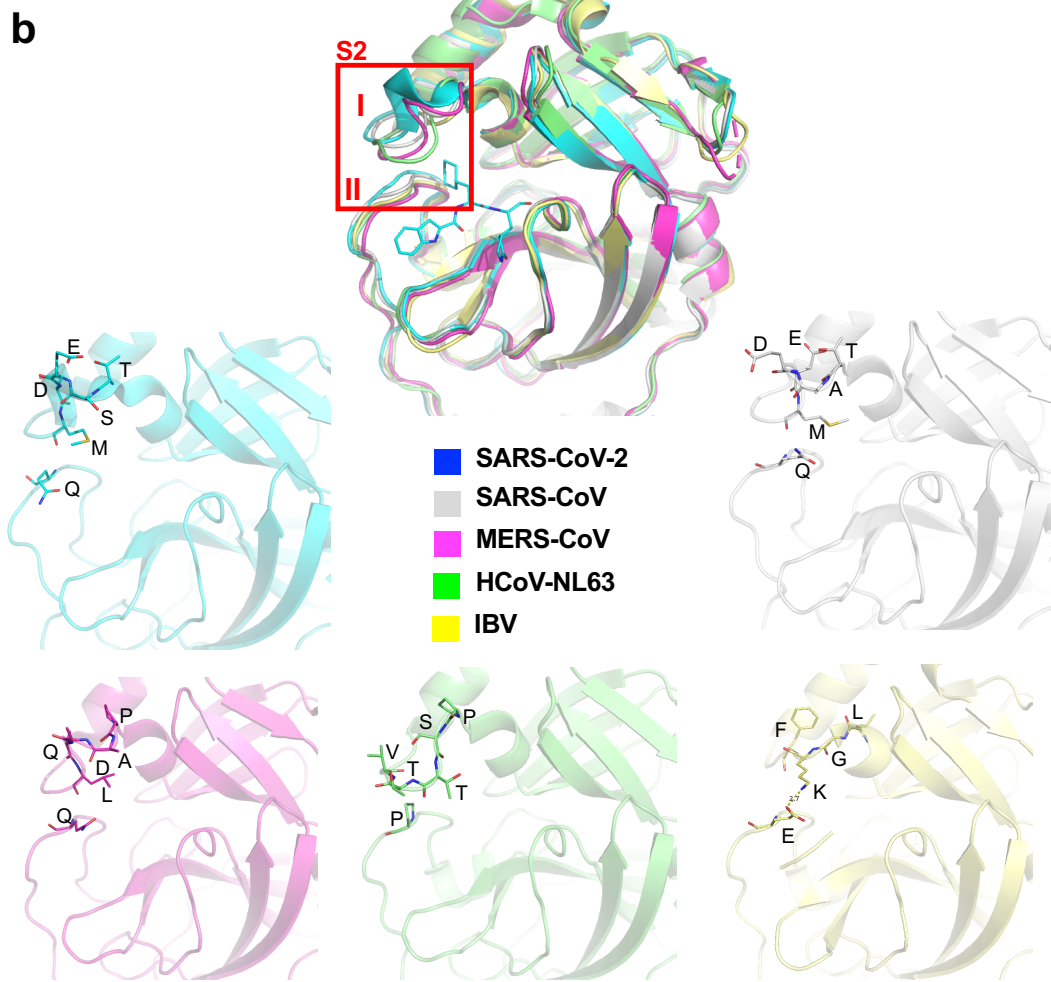
54 (in place of threonine). Structures were obtained from the Protein Data Bank: SARS-CoV-2 (PDB: 6LZE),

55 SARS-CoV (PDB: 2HOB), MERS-CoV (PDB: 5WKJ), HCoV-NL63 (PDB: 5GWY), and IBV (PDB: 2Q6F).

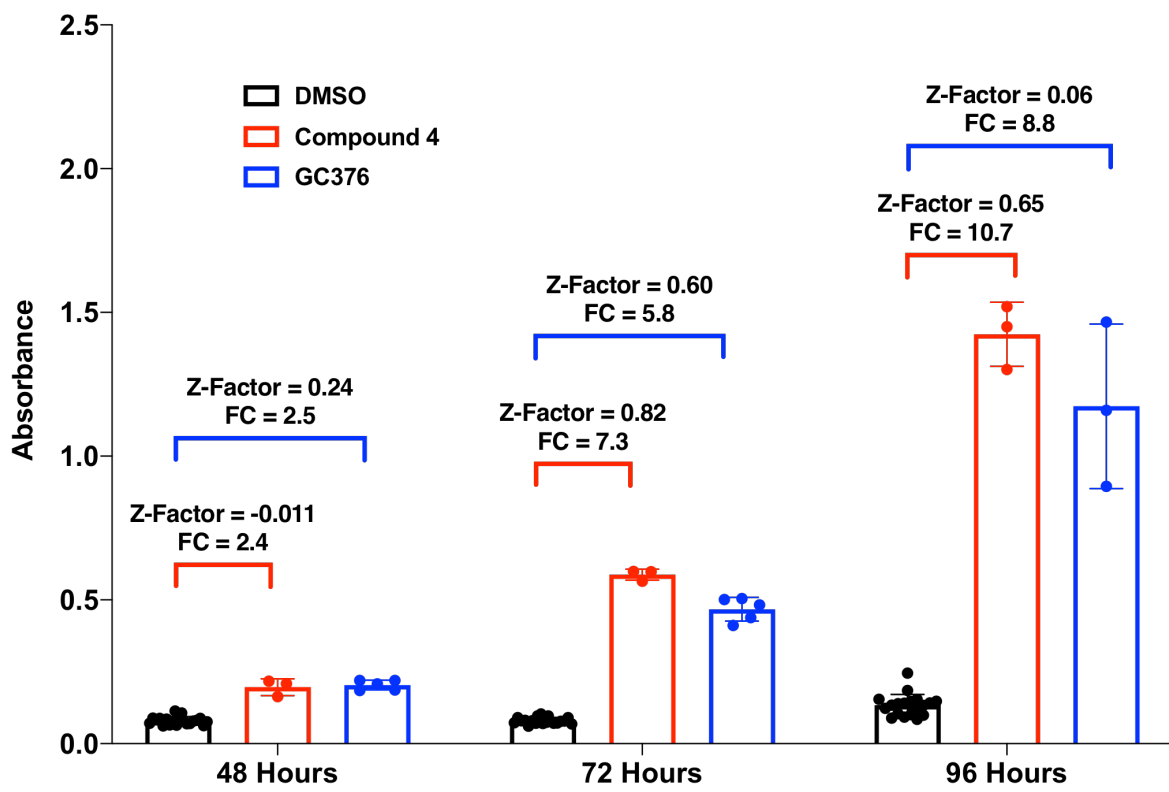
56 The sequence for Bat-CoV-HKU9 was obtained from P0C6W5 (R1AB_BCHK9) in UniProt.

a

SARS-CoV-2	5	10	15	20	25	30	35	40	45	50	55	60	65	70	75	80	85	90	95			
SARS-CoV	~~~	SGFRKNAFPGKVCGVQVTCGTTLNGLWLDGVV	10	15	20	25	30	35	40	45	50	55	60	65	70	75	80	85	90	95		
MERS-CoV	1	~~~SGFRKNAFPGKVCGVQVTCGTTLNGLWLDGVV	10	15	20	25	30	35	40	45	50	55	60	65	70	75	80	85	90	95		
Bat-CoV-HKU9	-1	~~~HHSCLVKMSHPGCGVTEACMVQVTCGSMTLNGIWLDNTV	10	15	20	25	30	35	40	45	50	55	60	65	70	75	80	85	90	95		
HCoV-NL63	1	SPPCWAGLTRMAMPGSLVPECLVKVNYYGNSMILNGIWLDNTV	10	15	20	25	30	35	40	45	50	55	60	65	70	75	80	85	90	95		
IBV	3	~~~~~LRKMAQPSGCVERCVWRVCYGSTVLNGWLGDV	5	10	15	20	25	30	35	40	45	50	55	60	65	70	75	80	85	90	95	
SARS-CoV-2	1	~~~SGFKLVLSPSSAVERCVSVSYRGNLNLGWLGS	10	15	20	25	30	35	40	45	50	55	60	65	70	75	80	85	90	95		
SARS-CoV	100	KYKFRIOPGTFSVLACYNGSPSGVYOCAMRNFTIKGSFLNGSCGSGVFNIDYD	105	110	115	120	125	130	135	140	145	150	155	160	165	170	175	180	185	190	195	200
MERS-CoV	100	KYKFRIOPGTFSVLACYNGSPSGVYOCAMRNFTIKGSFLNGSCGSGVFNIDYD	105	110	115	120	125	130	135	140	145	150	155	160	165	170	175	180	185	190	195	200
Bat-CoV-HKU9	103	AVTTFTVKPQAAFSVLACYNGSPGTYGRPTGFTTVNRYTTIKGSFLNGSCGSGVFNIDYD	108	110	115	120	125	130	135	140	145	150	155	160	165	170	175	180	185	190	195	200
HCoV-NL63	3508	ANXPIFVRSVTGOMSLLADYGLPTGVVCTLNGSCGSGVFNIDYD	3510	3515	3520	3525	3530	3535	3540	3545	3550	3555	3560	3565	3570	3575	3580	3585	3590	3595	3600	3605
IBV	99	KHVFKTLEKEGDSFTIACSYGTVNLACEYGIASGYFGVNLRTNFTIKGSFINGAACGGSPGYNVNRNDGTCTEVCFYLHQI	100	105	110	115	120	125	130	135	140	145	150	155	160	165	170	175	180	185	190	195
SARS-CoV-2	204	VLAWLVAAVINGDRWNFLNRPTTTLNDFLNLVAMKYNNPEPLTDQHVDILGPLS	205	210	215	220	225	230	235	240	245	250	255	260	265	270	275	280	285	290	295	300
SARS-CoV	204	VLAWLVAAVINGDRWNFLNRPTTTLNDFLNLVAMKYNNPEPLTDQHVDILGPLS	205	210	215	220	225	230	235	240	245	250	255	260	265	270	275	280	285	290	295	300
MERS-CoV	207	VVANLYAALINGCANFVKPNTSVUSNEWALANOFTEFGV	3612	3615	3620	3625	3630	3635	3640	3645	3650	3655	3660	3665	3670	3675	3680	3685	3690	3695	3700	3710
Bat-CoV-HKU9	204	VVAPFLTAAILNGCRWNWSTRVWDGFNEWAANGTYTVWS	205	210	215	220	225	230	235	240	245	250	255	260	265	270	275	280	285	290	295	300
HCoV-NL63	204	IVANLYAAIIISPKWLES-TTVSIEDYINRWSASDNGFTPST	205	210	215	220	225	230	235	240	245	250	255	260	265	270	275	280	285	290	295	300
IBV	202	IVANLYAAIIISPKWLES-TTVSIEDYINRWSASDNGFTPST	202	205	210	215	220	225	230	235	240	245	250	255	260	265	270	275	280	285	290	295

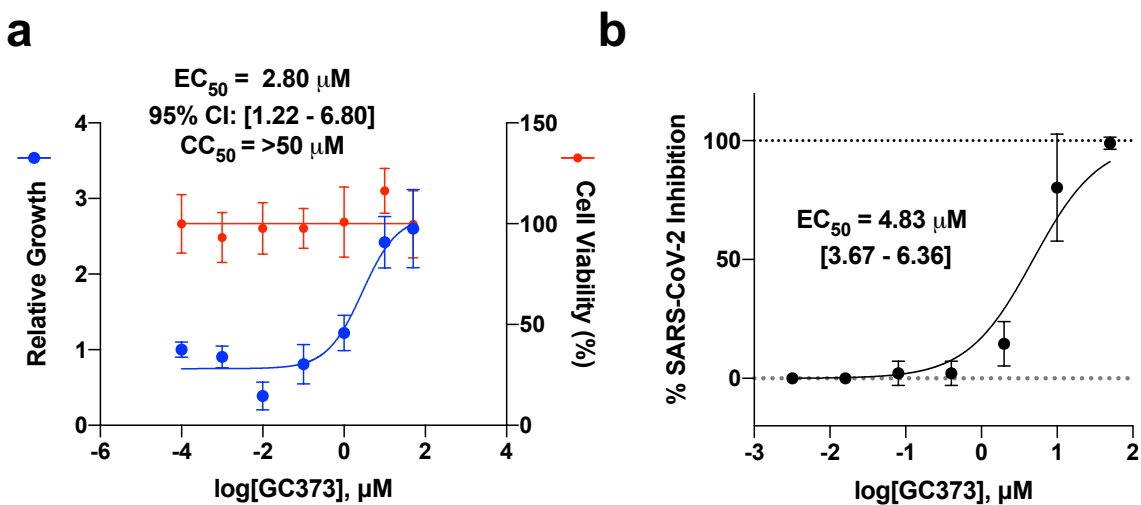


58 **Supplementary Fig. 7. Optimization of screening parameters and resulting Z-factors between**
 59 **positive and negative control wells.** Z-factor, a measure of assay quality was determined for two positive
 60 control compounds, GC376 at 50 μ M and compound 4 at 20 μ M, at different time points to identify optimal
 61 screening conditions for compounds against the SARS-CoV-2-3CLpro. The DMSO condition was conducted
 62 with 21 technical replicates randomly positioned across a 96-well plate while positive control compounds
 63 were tested at three or five technical replicates. FC = Fold Change. Data are shown as mean \pm s.d. for
 64 specified technical replicates.



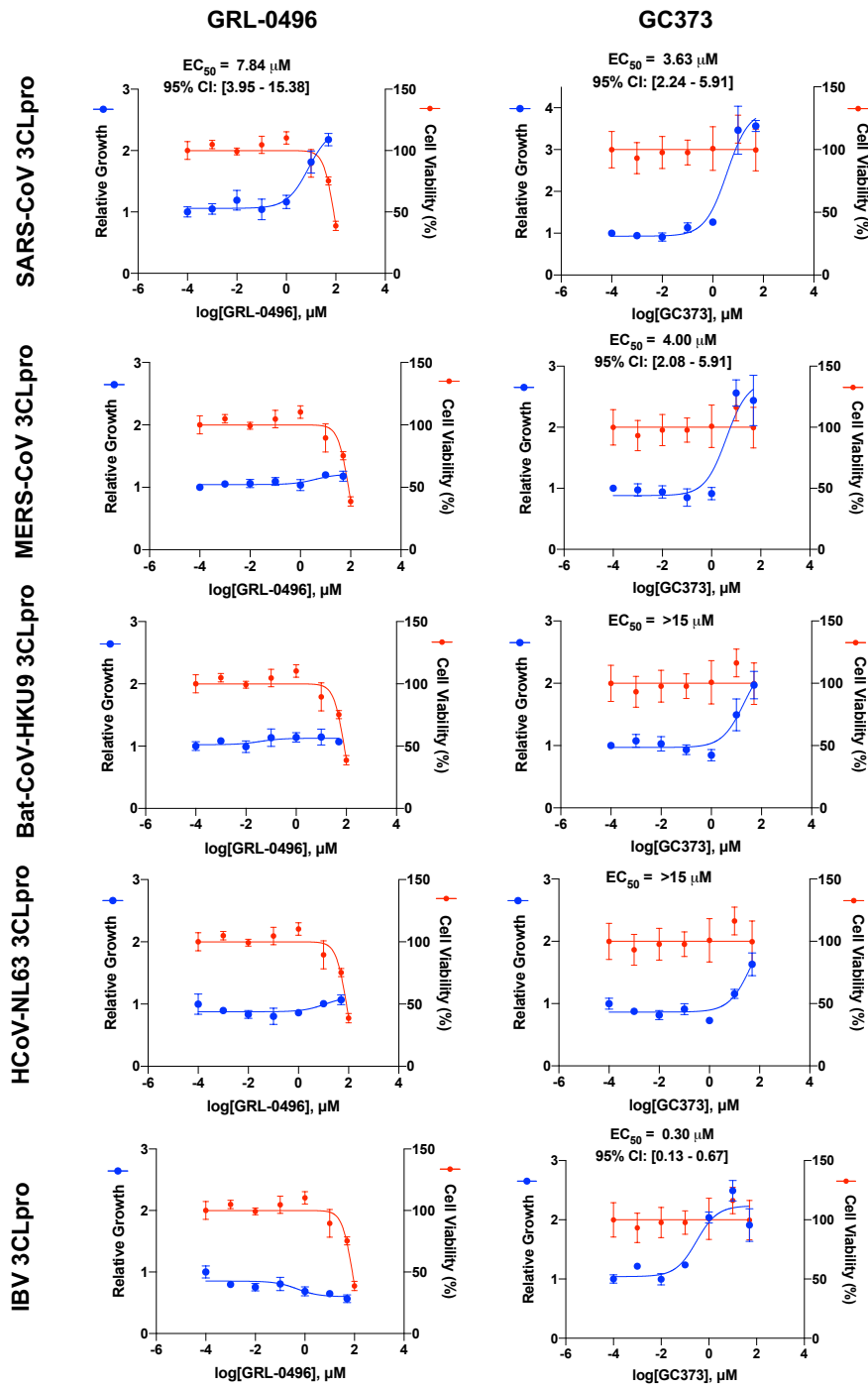
65
 66
 67

68 **Supplementary Fig. 8. GC373 demonstrates activity against the SARS-CoV-2 3CLpro and against the**
 69 **SARS-CoV-2 live virus.** **a.** Dose-response profiling and cytotoxicity determination using the transfection-
 70 based assay of GC373 against the SARS-CoV-2 3CLpro. **b.** Live virus testing of GC373 against SARS-CoV-
 71 2. EC₅₀ values are displayed as best-fit value alongside 95% confidence interval. The live virus assay was
 72 conducted with two biological replicates, each with three technical replicates and the EC₅₀ value was derived
 73 from all replicates. CC₅₀ values are displayed as best-fit value. Data are shown as mean ± s.d. for three or
 74 four technical replicates.



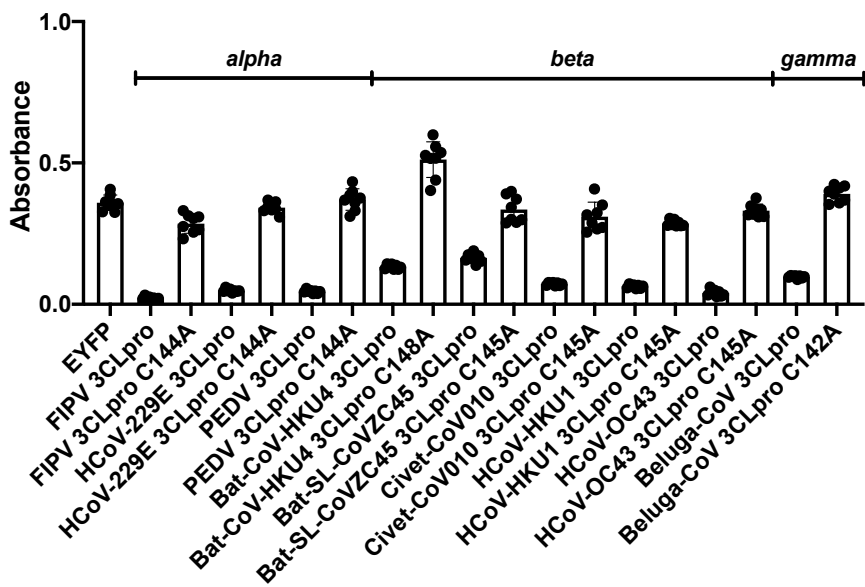
75
 76

77 **Supplementary Fig. 9. The activity of GRL-0496 and GC373 show variable efficacy and potency**
 78 **against the coronavirus 3CL proteases from SARS-CoV, MERS-CoV, Bat-CoV-HKU9, HCoV-NL63,**
 79 **and IBV. EC₅₀ values are displayed as best-fit value alongside 95% confidence interval. CC₅₀ values are**
 80 **displayed as best-fit value. Data are shown as mean ± s.d. for four technical replicates.**



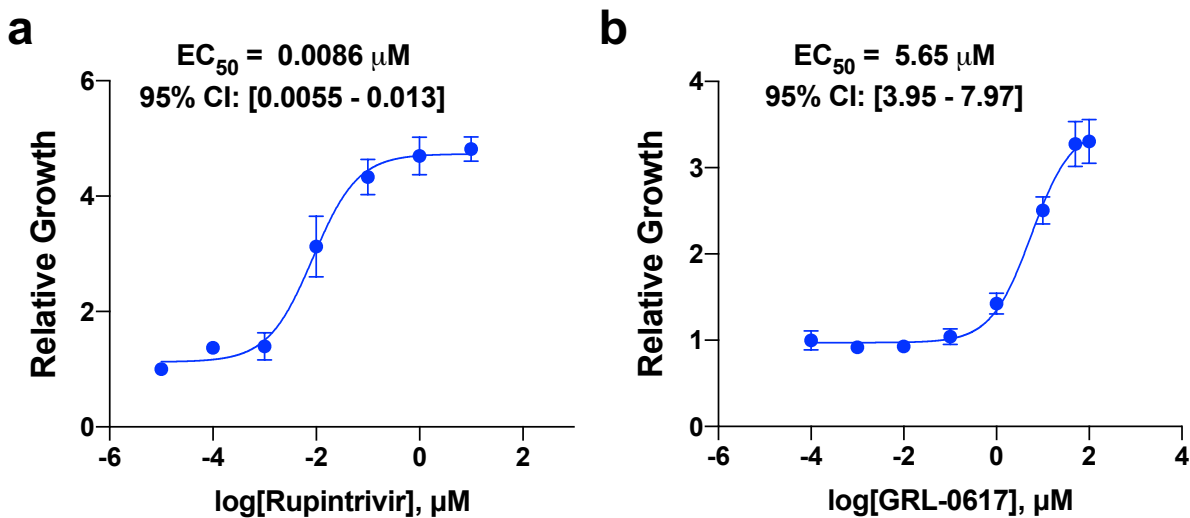
81
 82

83 **Supplementary Fig. 10. Expression of multiple other coronavirus 3CLpros results in protease-
84 mediated cytotoxicity.** Quantification of cytotoxicity upon expression of active or inactivated 3CLpro
85 enzymes from FIPV, HCoV-229E, PEDV, Bat-CoV-HKU4, Bat-SL-CoVZC45, Civet-Cov010, HCoV-HKU1,
86 HCoV-OC43, and Beluga-CoV in 293T cells. Data are shown as mean \pm s.d. for eight technical replicates.
87 The genus from which each protease is derived is listed above the bar graphs.



88

89 **Supplementary Fig. 11. Expression of 3C proteases and papain-like proteases within cells causes**
90 **cytotoxicity that can be rescued by known inhibitors.** **a.** Dose-response profiling of Rupintrivir against
91 HRV-B14 3C protease using the transfection-based assay. **b.** Dose-response profiling of GRL-0617 against
92 SARS-CoV PLP using the transfection-based assay. EC₅₀ values are displayed as best-fit value alongside
93 95% confidence interval. Data are shown as mean ± s.d. for three or four technical replicates.



94

95 **Supplementary Table 1. Selectivity Index (SI) for compounds tested with the transfection-based**
 96 **assay in this study.**

Protease	Drug	EC ₅₀ (μM)	CC ₅₀ (μM)	SI (CC ₅₀ /EC ₅₀)
SARS-CoV-2 3CLpro	GC376	3.30	>100	>30.3
	compound 4	0.98	81	82.7
	11a	6.89	48	7.0
	GRL-0496	5.05	81	16.0
	GC373	2.80	>50	>17.9
	SL-4-241	7.15	>100	>14.0
SARS-CoV 3CLpro	GC376	5.83	>100	>17.2
	compound 4	3.17	81	25.6
	11a	5.38	48	8.9
	GRL-0496	7.84	81	10.3
	GC373	3.63	>50	>13.8
MERS-CoV 3CLpro	GC376	7.44	>100	>13.4
	compound 4	1.40	81	57.9
	GC373	4.00	>50	>12.5
Bat-CoV-HKU9 3CLpro	GC376	11.07	>100	>9.0
	compound 4	4.11	81	19.7
HCoV-NL63 3CLpro	compound 4	4.92	81	16.5
IBV 3CLpro	GC376	0.58	>100	>172.0
	compound 4	0.058	81	1396.5
	GC373	0.30	>50	>166.6
Bat-SL-CoVZC45 3CLpro	GC376	2.08	>100	>48.1
	compound 4	2.53	81	32.0
Bat-CoV-HKU4 3CLpro	GC376	3.33	>100	>30.0
	compound 4	3.24	81	25.0
HCoV-OC43 3CLpro	GC376	7.13	>100	>14.0
HCoV-HKU1 3CLpro	GC376	6.92	>100	>14.5
	compound 4	2.64	81	30.7
HCoV-229E 3CLpro	GC376	7.51	>100	>13.3
Beluga-CoV 3CLpro	GC376	4.72	>100	>21.2
	compound 4	2.51	81	32.3
FIPV 3CLpro	GC376	5.27	>100	>19.0
	compound 4	4.19	81	19.3
PEDV 3CLpro	GC376	8.88	>100	>11.3
	compound 4	1.61	81	50.2
Civet-CoV010 3CLpro	GC376	6.27	>100	>15.9
	compound 4	3.69	81	21.0

97

98

Supplementary Table 2. Compounds screened for activity against the SARS-CoV-2 3CLpro.

Absorbance	Well	Drug	Plate	Model	z-score
0.07156	A02	Omarigliptin	Plate1	SARS-CoV-2 3CLpro	0.07462451
0.03996	A03	Apoptosis Activator 2	Plate1	SARS-CoV-2 3CLpro	-3.5532747
0.06801	A04	Picolamine	Plate1	SARS-CoV-2 3CLpro	-0.3329401
0.07551	A05	Muscone	Plate1	SARS-CoV-2 3CLpro	0.52811191
0.08101	A06	2-Aminoethanethiol	Plate1	SARS-CoV-2 3CLpro	1.15955007
0.07101	A07	Dexibuprofen	Plate1	SARS-CoV-2 3CLpro	0.01148069
0.07496	A08	Glucosamine	Plate1	SARS-CoV-2 3CLpro	0.4649681
0.07141	A09	Gabexate mesylate	Plate1	SARS-CoV-2 3CLpro	0.05740347
0.09891	A10	Zalcitabine	Plate1	SARS-CoV-2 3CLpro	3.21459426
0.09016	A11	Amiloride hydrochloride	Plate1	SARS-CoV-2 3CLpro	2.21003355
0.06776	B02	Saxagliptin hydrate	Plate1	SARS-CoV-2 3CLpro	-0.3616419
0.07901	B03	Linagliptin	Plate1	SARS-CoV-2 3CLpro	0.9299362
0.07831	B04	Sitagliptin	Plate1	SARS-CoV-2 3CLpro	0.84957134
0.08006	B05	Hexylresorcinol	Plate1	SARS-CoV-2 3CLpro	1.05048348
0.06906	B06	Arbutin	Plate1	SARS-CoV-2 3CLpro	-0.2123928
0.03171	B07	Diminazene Aceturate	Plate1	SARS-CoV-2 3CLpro	-4.500432
0.06266	B08	3-Pyridylacetic acid hydrochloride	Plate1	SARS-CoV-2 3CLpro	-0.9471572
0.05386	B09	Racecadotril	Plate1	SARS-CoV-2 3CLpro	-1.9574583
0.06456	B10	Mizoribine	Plate1	SARS-CoV-2 3CLpro	-0.7290241
0.08056	B11	Sodium etidronate	Plate1	SARS-CoV-2 3CLpro	1.10788695
0.07191	C02	MAC-5576	Plate1	SARS-CoV-2 3CLpro	0.11480694
0.07666	C03	DMSO	Plate1	SARS-CoV-2 3CLpro	0.66013989
0.07206	C04	DMSO	Plate1	SARS-CoV-2 3CLpro	0.13202798
0.07451	C05	DMSO	Plate1	SARS-CoV-2 3CLpro	0.41330498
0.07591	C06	BTB07404	Plate1	SARS-CoV-2 3CLpro	0.57403469
0.06836	C07	DMSO	Plate1	SARS-CoV-2 3CLpro	-0.2927577
0.06826	C08	DMSO	Plate1	SARS-CoV-2 3CLpro	-0.3042384
0.07401	C09	Myrecetin	Plate1	SARS-CoV-2 3CLpro	0.35590151
0.06881	C10	DMSO	Plate1	SARS-CoV-2 3CLpro	-0.2410946
0.08486	C11	Tipranivir	Plate1	SARS-CoV-2 3CLpro	1.60155678
0.06106	D02	DMSO	Plate1	SARS-CoV-2 3CLpro	-1.1308483
0.06566	D03	BTB07408	Plate1	SARS-CoV-2 3CLpro	-0.6027364
0.36221	D04	GC376	Plate1	SARS-CoV-2 3CLpro	33.443261
0.06851	D05	MAC-8120	Plate1	SARS-CoV-2 3CLpro	-0.2755367
0.06866	D06	DMSO	Plate1	SARS-CoV-2 3CLpro	-0.2583156
0.07186	D07	MWP00332	Plate1	SARS-CoV-2 3CLpro	0.10906659

0.07301	D08	DMSO	Plate1	SARS-CoV-2 3CLpro	0.24109457
0.07556	D09	DMSO	Plate1	SARS-CoV-2 3CLpro	0.53385226
0.07011	D10	Rupintrivir	Plate1	SARS-CoV-2 3CLpro	-0.0918456
0.06876	D11	DMSO	Plate1	SARS-CoV-2 3CLpro	-0.2468349
0.06221	E02	DMSO	Plate1	SARS-CoV-2 3CLpro	-0.9988204
0.06836	E03	DMSO	Plate1	SARS-CoV-2 3CLpro	-0.2927577
0.06486	E04	BTB07417	Plate1	SARS-CoV-2 3CLpro	-0.694582
0.07096	E05	DMSO	Plate1	SARS-CoV-2 3CLpro	0.00574035
0.06971	E06	AZVIII-49F	Plate1	SARS-CoV-2 3CLpro	-0.1377683
0.06231	E07	DMSO	Plate1	SARS-CoV-2 3CLpro	-0.9873397
0.07276	E08	MWP00508	Plate1	SARS-CoV-2 3CLpro	0.21239284
0.06846	E09	DMSO	Plate1	SARS-CoV-2 3CLpro	-0.281277
0.06741	E10	DMSO	Plate1	SARS-CoV-2 3CLpro	-0.4018243
0.07371	E11	MWP00333	Plate1	SARS-CoV-2 3CLpro	0.32145943
0.04971	F02	Grazoprevir	Plate1	SARS-CoV-2 3CLpro	-2.4339071
0.06991	F03	AZVIII-57D	Plate1	SARS-CoV-2 3CLpro	-0.1148069
0.06831	F04	DMSO	Plate1	SARS-CoV-2 3CLpro	-0.298498
0.06911	F05	BTB07407	Plate1	SARS-CoV-2 3CLpro	-0.2066525
0.07516	F06	DMSO	Plate1	SARS-CoV-2 3CLpro	0.48792949
0.47481	F07	CMPD18-20	Plate1	SARS-CoV-2 3CLpro	46.3705222
0.07086	F08	DMSO	Plate1	SARS-CoV-2 3CLpro	-0.0057403
0.18266	F09	GRL-0496	Plate1	SARS-CoV-2 3CLpro	12.8296753
0.05571	F10	Saquinavir	Plate1	SARS-CoV-2 3CLpro	-1.7450655
0.06161	F11	DMSO	Plate1	SARS-CoV-2 3CLpro	-1.0677045
0.04941	G02	Monobenzone	Plate1	SARS-CoV-2 3CLpro	-2.4683492
0.08226	G03	Limonin	Plate1	SARS-CoV-2 3CLpro	1.30305874
0.02596	G04	Betulinic acid	Plate1	SARS-CoV-2 3CLpro	-5.1605719
0.07796	G05	PMSF	Plate1	SARS-CoV-2 3CLpro	0.80938891
0.08286	G06	Fenofibric acid	Plate1	SARS-CoV-2 3CLpro	1.37194291
0.07241	G07	Ramelteon	Plate1	SARS-CoV-2 3CLpro	0.17221041
0.05871	G08	Ritonavir	Plate1	SARS-CoV-2 3CLpro	-1.4006446
0.08216	G09	Alogliptin Benzoate	Plate1	SARS-CoV-2 3CLpro	1.29157805
0.00986	G10	Bortezomib	Plate1	SARS-CoV-2 3CLpro	-7.0089636
0.08641	G11	Acetohydroxamic acid	Plate1	SARS-CoV-2 3CLpro	1.77950754
0.07081	H02	Nevirapine	Plate1	SARS-CoV-2 3CLpro	-0.0114807
0.05576	H03	Lopinavir	Plate1	SARS-CoV-2 3CLpro	-1.7393251
0.07581	H04	Penciclovir	Plate1	SARS-CoV-2 3CLpro	0.562554
0.01181	H05	AOB2796	Plate1	SARS-CoV-2 3CLpro	-6.78509
0.08421	H06	Maribavir	Plate1	SARS-CoV-2 3CLpro	1.52693227

0.08156	H07	Trelagliptin succinate	Plate1	SARS-CoV-2 3CLpro	1.22269389
0.01741	H08	MLN9708	Plate1	SARS-CoV-2 3CLpro	-6.1421712
0.07691	H09	SC514	Plate1	SARS-CoV-2 3CLpro	0.68884163
0.01011	H10	Ixazomib	Plate1	SARS-CoV-2 3CLpro	-6.9802618
0.08826	H11	Raltegravir potassium	Plate1	SARS-CoV-2 3CLpro	1.99190037
0.082225	A02	PSI6206	Plate2	SARS-CoV-2 3CLpro	0.48063475
0.069275	A03	Cilastatin	Plate2	SARS-CoV-2 3CLpro	-0.3492612
0.068975	A04	Taxifolin	Plate2	SARS-CoV-2 3CLpro	-0.3684866
0.084325	A05	Nafamostat mesylate	Plate2	SARS-CoV-2 3CLpro	0.61521247
0.047775	A06	Daclatasvir dihydrochloride	Plate2	SARS-CoV-2 3CLpro	-1.7270809
0.094525	A07	Darunavir†Ethanolate	Plate2	SARS-CoV-2 3CLpro	1.26887573
0.106675	A08	Ilomastat	Plate2	SARS-CoV-2 3CLpro	2.04750402
0.049625	A09	Elvitegravir	Plate2	SARS-CoV-2 3CLpro	-1.6085243
0.076575	A10	Dolutegravir sodium	Plate2	SARS-CoV-2 3CLpro	0.11855657
0.108725	A11	Astragaloside IV	Plate2	SARS-CoV-2 3CLpro	2.17887751
0.064175	B02	Arctigenin	Plate2	SARS-CoV-2 3CLpro	-0.6760929
0.086575	B03	Stigmasterol	Plate2	SARS-CoV-2 3CLpro	0.7594029
0.054075	B04	Nobiletin	Plate2	SARS-CoV-2 3CLpro	-1.3233477
0.005175	B05	Celastrol	Plate2	SARS-CoV-2 3CLpro	-4.4570862
0.093275	B06	Glucosamine sulfate	Plate2	SARS-CoV-2 3CLpro	1.18876994
0.068025	B07	Picroside I	Plate2	SARS-CoV-2 3CLpro	-0.429367
0.078775	B08	Alvelestat	Plate2	SARS-CoV-2 3CLpro	0.25954276
0.079225	B09	N-Ethylmaleimide	Plate2	SARS-CoV-2 3CLpro	0.28838085
0.068525	B10	DAPT	Plate2	SARS-CoV-2 3CLpro	-0.3973247
0.103975	B11	Trelagliptin	Plate2	SARS-CoV-2 3CLpro	1.87447551
0.085725	C02	Fosamprenavir	Plate2	SARS-CoV-2 3CLpro	0.70493096
0.057525	C03	DMSO	Plate2	SARS-CoV-2 3CLpro	-1.1022557
0.056875	C04	DMSO	Plate2	SARS-CoV-2 3CLpro	-1.1439107
0.060275	C05	Indinavir	Plate2	SARS-CoV-2 3CLpro	-0.9260229
0.081325	C06	DMSO	Plate2	SARS-CoV-2 3CLpro	0.42295858
0.085675	C07	DMSO	Plate2	SARS-CoV-2 3CLpro	0.70172673
0.726225	C08	CMPD18-20	Plate2	SARS-CoV-2 3CLpro	41.7511382
0.067575	C09	DMSO	Plate2	SARS-CoV-2 3CLpro	-0.4582051
0.117025	C10	SPB08384	Plate2	SARS-CoV-2 3CLpro	2.71077996
0.123825	C11	DMSO	Plate2	SARS-CoV-2 3CLpro	3.14655547
0.085025	D02	DMSO	Plate2	SARS-CoV-2 3CLpro	0.66007172
0.486725	D03	CMPD18-10	Plate2	SARS-CoV-2 3CLpro	26.40286868
0.074775	D04	DMSO	Plate2	SARS-CoV-2 3CLpro	0.00320423

0.075325	D05	DMSO	Plate2	SARS-CoV-2 3CLpro	0.03845078
0.088475	D06	Apigenin	Plate2	SARS-CoV-2 3CLpro	0.8811637
0.080225	D07	AZVIII-57G	Plate2	SARS-CoV-2 3CLpro	0.35246548
0.060775	D08	DMSO	Plate2	SARS-CoV-2 3CLpro	-0.8939806
0.066125	D09	SPB06613	Plate2	SARS-CoV-2 3CLpro	-0.5511278
0.074225	D10	DMSO	Plate2	SARS-CoV-2 3CLpro	-0.0320423
0.113225	D11	SPB06636	Plate2	SARS-CoV-2 3CLpro	2.46725836
0.071675	E02	AZVIII-38	Plate2	SARS-CoV-2 3CLpro	-0.1954581
0.083175	E03	DMSO	Plate2	SARS-CoV-2 3CLpro	0.54151515
0.073475	E04	AZVIII-49C	Plate2	SARS-CoV-2 3CLpro	-0.0801058
0.085225	E05	DMSO	Plate2	SARS-CoV-2 3CLpro	0.67288864
0.070925	E06	Quercetin	Plate2	SARS-CoV-2 3CLpro	-0.2435216
0.078575	E07	DMSO	Plate2	SARS-CoV-2 3CLpro	0.24672584
0.073625	E08	SPB06591	Plate2	SARS-CoV-2 3CLpro	-0.0704931
0.076475	E09	DMSO	Plate2	SARS-CoV-2 3CLpro	0.11214811
0.077875	E10	SPB06593	Plate2	SARS-CoV-2 3CLpro	0.20186659
0.117725	E11	DMSO	Plate2	SARS-CoV-2 3CLpro	2.75563921
0.074675	F02	DMSO	Plate2	SARS-CoV-2 3CLpro	-0.0032042
0.060375	F03	DMSO	Plate2	SARS-CoV-2 3CLpro	-0.9196145
0.077325	F04	DMSO	Plate2	SARS-CoV-2 3CLpro	0.16662005
0.078525	F05	Famotidine	Plate2	SARS-CoV-2 3CLpro	0.2435216
0.071325	F06	DMSO	Plate2	SARS-CoV-2 3CLpro	-0.2178878
0.412325	F07	GC376	Plate2	SARS-CoV-2 3CLpro	21.634972
0.070025	F08	DMSO	Plate2	SARS-CoV-2 3CLpro	-0.3011978
0.068675	F09	DMSO	Plate2	SARS-CoV-2 3CLpro	-0.387712
0.076275	F10	DMSO	Plate2	SARS-CoV-2 3CLpro	0.09933118
0.096375	F11	DMSO	Plate2	SARS-CoV-2 3CLpro	1.3874323
0.071175	G02	Z-VAD(OMe)-FMK	Plate2	SARS-CoV-2 3CLpro	-0.2275004
0.076225	G03	Abietic Acid	Plate2	SARS-CoV-2 3CLpro	0.09612695
0.061225	G04	Atazanavir sulfate	Plate2	SARS-CoV-2 3CLpro	-0.8651425
0.089475	G05	Abacavir	Plate2	SARS-CoV-2 3CLpro	0.94524833
0.056675	G06	Balicatib	Plate2	SARS-CoV-2 3CLpro	-1.1567276
0.011625	G07	Carfilzomib	Plate2	SARS-CoV-2 3CLpro	-4.0437403
0.054975	G08	Atazanavir	Plate2	SARS-CoV-2 3CLpro	-1.2656715
0.068275	G09	Vildagliptin	Plate2	SARS-CoV-2 3CLpro	-0.4133459
0.025775	G10	Dapivirine	Plate2	SARS-CoV-2 3CLpro	-3.1369428
0.072375	G11	SB-3CT	Plate2	SARS-CoV-2 3CLpro	-0.1505989
0.060825	H02	PD 151746	Plate2	SARS-CoV-2 3CLpro	-0.8907764
0.018775	H03	PAC1	Plate2	SARS-CoV-2 3CLpro	-3.5855352

0.073725	H04	Camostat mesilate	Plate2	SARS-CoV-2 3CLpro	-0.0640846
0.073525	H05	Efavirenz	Plate2	SARS-CoV-2 3CLpro	-0.0769016
0.088325	H06	Des(benzylpyridyl) Atazanavir	Plate2	SARS-CoV-2 3CLpro	0.87155101
0.073375	H07	LY2811376	Plate2	SARS-CoV-2 3CLpro	-0.0865143
0.013175	H08	FLI06	Plate2	SARS-CoV-2 3CLpro	-3.9444091
0.056425	H09	SRPIN340	Plate2	SARS-CoV-2 3CLpro	-1.1727488
0.096125	H10	NSC 405020	Plate2	SARS-CoV-2 3CLpro	1.37141114
0.088525	H11	Leupeptin Hemisulfate	Plate2	SARS-CoV-2 3CLpro	0.88436793
0.01024	A02	Epoxomicin	Plate3	SARS-CoV-2 3CLpro	-4.8596643
0.02879	A03	MG101	Plate3	SARS-CoV-2 3CLpro	-3.6239306
0.06649	A04	lavendustin C	Plate3	SARS-CoV-2 3CLpro	-1.1124934
0.08099	A05	BMS707035	Plate3	SARS-CoV-2 3CLpro	-0.146556
0.05509	A06	Asunaprevir	Plate3	SARS-CoV-2 3CLpro	-1.87192
0.07839	A07	Loxistatin Acid	Plate3	SARS-CoV-2 3CLpro	-0.3197586
0.00484	A08	GK921	Plate3	SARS-CoV-2 3CLpro	-5.2193927
0.06729	A09	L-685,458	Plate3	SARS-CoV-2 3CLpro	-1.0592003
0.07469	A10	Tenofovir Disoproxil Fumarate	Plate3	SARS-CoV-2 3CLpro	-0.5662392
0.02539	A11	GSK690693	Plate3	SARS-CoV-2 3CLpro	-3.8504263
0.03379	B02	Ledipasvir	Plate3	SARS-CoV-2 3CLpro	-3.2908487
0.01554	B03	ONX0914	Plate3	SARS-CoV-2 3CLpro	-4.5065975
0.06614	B04	PI1840	Plate3	SARS-CoV-2 3CLpro	-1.1358091
0.08239	B05	(+)-Isocorydine hydrochloride	Plate3	SARS-CoV-2 3CLpro	-0.0532931
0.09179	B06	UAMC 00039 dihydrochloride	Plate3	SARS-CoV-2 3CLpro	0.57290079
0.01119	B07	PE859	Plate3	SARS-CoV-2 3CLpro	-4.7963787
0.08269	B08	RO4929097	Plate3	SARS-CoV-2 3CLpro	-0.0333082
0.09519	B09	Emricasan	Plate3	SARS-CoV-2 3CLpro	0.79939646
0.07204	B10	CGS 27023A	Plate3	SARS-CoV-2 3CLpro	-0.7427725
0.08719	B11	Talabostat mesylate	Plate3	SARS-CoV-2 3CLpro	0.26646549
0.09014	C02	AZVIII-33B	Plate3	SARS-CoV-2 3CLpro	0.46298378
0.07829	C03	DMSO	Plate3	SARS-CoV-2 3CLpro	-0.3264202
0.07454	C04	MDL28170	Plate3	SARS-CoV-2 3CLpro	-0.5762316
0.08274	C05	DMSO	Plate3	SARS-CoV-2 3CLpro	-0.0299774
0.08389	C06	DMSO	Plate3	SARS-CoV-2 3CLpro	0.04663146
0.09039	C07	AZVIII-44H	Plate3	SARS-CoV-2 3CLpro	0.47963787
0.08804	C08	DMSO	Plate3	SARS-CoV-2 3CLpro	0.3230894
0.08794	C09	DMSO	Plate3	SARS-CoV-2 3CLpro	0.31642776
0.08059	C10	DMSO	Plate3	SARS-CoV-2 3CLpro	-0.1732026

0.07924	C11	DMSO	Plate3	SARS-CoV-2 3CLpro	-0.2631347
0.08329	D02	DMSO	Plate3	SARS-CoV-2 3CLpro	0.00666164
0.07209	D03	Bicailein	Plate3	SARS-CoV-2 3CLpro	-0.7394417
0.50684	D04	CMPD18-20	Plate3	SARS-CoV-2 3CLpro	28.2220257
0.23874	D05	GC373	Plate3	SARS-CoV-2 3CLpro	10.3621766
0.07824	D06	DMSO	Plate3	SARS-CoV-2 3CLpro	-0.329751
0.08409	D07	DMSO	Plate3	SARS-CoV-2 3CLpro	0.05995473
0.10644	D08	AZVIII-41A	Plate3	SARS-CoV-2 3CLpro	1.54883063
0.44099	D09	GC376	Plate3	SARS-CoV-2 3CLpro	23.8353377
0.09614	D10	DMSO	Plate3	SARS-CoV-2 3CLpro	0.86268201
0.04954	D11	MWP00709	Plate3	SARS-CoV-2 3CLpro	-2.2416409
0.02289	E02	NT 1-32	Plate3	SARS-CoV-2 3CLpro	-4.0169672
0.09329	E03	DMSO	Plate3	SARS-CoV-2 3CLpro	0.67282535
0.08949	E04	GRL0617	Plate3	SARS-CoV-2 3CLpro	0.41968314
0.09009	E05	DMSO	Plate3	SARS-CoV-2 3CLpro	0.45965296
0.13364	E06	AZVIII-34D	Plate3	SARS-CoV-2 3CLpro	3.36079593
0.07969	E07	DMSO	Plate3	SARS-CoV-2 3CLpro	-0.2331573
0.08989	E08	DMSO	Plate3	SARS-CoV-2 3CLpro	0.44632969
0.09419	E09	DMSO	Plate3	SARS-CoV-2 3CLpro	0.73278008
0.10229	E10	AZVIII-30	Plate3	SARS-CoV-2 3CLpro	1.27237269
0.08209	E11	DMSO	Plate3	SARS-CoV-2 3CLpro	-0.073278
0.08309	F02	DMSO	Plate3	SARS-CoV-2 3CLpro	-0.0066616
0.08234	F03	AZVIII-37A	Plate3	SARS-CoV-2 3CLpro	-0.0566239
0.09354	F04	DMSO	Plate3	SARS-CoV-2 3CLpro	0.68947944
0.07304	F05	Betrixaban	Plate3	SARS-CoV-2 3CLpro	-0.6761562
0.08944	F06	DMSO	Plate3	SARS-CoV-2 3CLpro	0.41635232
0.08344	F07	AZVIII-43A	Plate3	SARS-CoV-2 3CLpro	0.01665409
0.00659	F08	MAC22272	Plate3	SARS-CoV-2 3CLpro	-5.102814
0.10049	F09	Amentoflavone	Plate3	SARS-CoV-2 3CLpro	1.15246322
0.09359	F10	DMSO	Plate3	SARS-CoV-2 3CLpro	0.69281026
0.09164	F11	DMSO	Plate3	SARS-CoV-2 3CLpro	0.56290834
0.02859	G02	Ledipasvir acetone	Plate3	SARS-CoV-2 3CLpro	-3.6372539
0.08679	G03	Batimastat	Plate3	SARS-CoV-2 3CLpro	0.23981894
0.03034	G04	TOFA	Plate3	SARS-CoV-2 3CLpro	-3.5206752
0.03934	G05	HZ1157	Plate3	SARS-CoV-2 3CLpro	-2.9211279
0.09814	G06	Abacavir sulfate	Plate3	SARS-CoV-2 3CLpro	0.99591475
0.09834	G07	Sivelestat	Plate3	SARS-CoV-2 3CLpro	1.00923803
0.05434	G08	Dasabuvir	Plate3	SARS-CoV-2 3CLpro	-1.9218823
0.07869	G09	Calycosin	Plate3	SARS-CoV-2 3CLpro	-0.2997737

0.09329	G10	4-Methoxysalicylaldehyde	Plate3	SARS-CoV-2 3CLpro	0.67282535
0.09294	G11	Sebacic acid	Plate3	SARS-CoV-2 3CLpro	0.64950962
0.07394	H02	Deoxyarbutin	Plate3	SARS-CoV-2 3CLpro	-0.6162014
0.10384	H03	2-5-dihydroxyacetophenone	Plate3	SARS-CoV-2 3CLpro	1.37562807
0.09194	H04	Oxyresveratrol	Plate3	SARS-CoV-2 3CLpro	0.58289325
0.09649	H05	Aloxistattin	Plate3	SARS-CoV-2 3CLpro	0.88599774
0.11434	H06	Fostemsavir	Plate3	SARS-CoV-2 3CLpro	2.07509997
0.07149	H07	Tasisulam	Plate3	SARS-CoV-2 3CLpro	-0.7794115
0.09304	H08	Semagacestat	Plate3	SARS-CoV-2 3CLpro	0.65617126
0.07974	H09	Triciribine	Plate3	SARS-CoV-2 3CLpro	-0.2298265
0.09534	H10	IMR-1A	Plate3	SARS-CoV-2 3CLpro	0.80938891
0.09124	H11	IMR1	Plate3	SARS-CoV-2 3CLpro	0.53626179
0.12075	A02	Z-IETD-FMK	Plate4	SARS-CoV-2 3CLpro	3.10166071
0.1	A03	VR23	Plate4	SARS-CoV-2 3CLpro	1.72277566
0.08645	A04	Amprenavir	Plate4	SARS-CoV-2 3CLpro	0.82234711
0.10545	A05	AA26-9	Plate4	SARS-CoV-2 3CLpro	2.08494065
0.04395	A06	Dolutegravir	Plate4	SARS-CoV-2 3CLpro	-2.0018753
0.0624	A07	Lomibuvir	Plate4	SARS-CoV-2 3CLpro	-0.7758305
0.05675	A08	Ginsenoside Rh2	Plate4	SARS-CoV-2 3CLpro	-1.151286
0.08095	A09	UK371804	Plate4	SARS-CoV-2 3CLpro	0.45685951
0.02685	A10	CA-074 methyl ester	Plate4	SARS-CoV-2 3CLpro	-3.1382095
0.0603	A11	ML281	Plate4	SARS-CoV-2 3CLpro	-0.9153803
0.1165	B02	CP 640186	Plate4	SARS-CoV-2 3CLpro	2.81923847
0.10795	B03	Hydroumbelllic acid	Plate4	SARS-CoV-2 3CLpro	2.25107138
0.084	B04	Ethyl gallate	Plate4	SARS-CoV-2 3CLpro	0.65953899
0.0811	B05	Senegenin	Plate4	SARS-CoV-2 3CLpro	0.46682735
0.0767	B06	lithospermic acid	Plate4	SARS-CoV-2 3CLpro	0.17443727
0.0637	B07	Dibenzazepine	Plate4	SARS-CoV-2 3CLpro	-0.6894425
0.0658	B08	LY411575	Plate4	SARS-CoV-2 3CLpro	-0.5498927
0.0668	B09	Paritaprevir	Plate4	SARS-CoV-2 3CLpro	-0.4834404
0.06765	B10	Sofosbuvir	Plate4	SARS-CoV-2 3CLpro	-0.426956
0.0935	B11	Crenigacestat	Plate4	SARS-CoV-2 3CLpro	1.29083576
0.11605	C02	Avagacestat	Plate4	SARS-CoV-2 3CLpro	2.78933494
0.1044	C03	Stearic acid	Plate4	SARS-CoV-2 3CLpro	2.01516574
0.09655	C04	DMSO	Plate4	SARS-CoV-2 3CLpro	1.49351525
0.5042	C05	CMPD18-20	Plate4	SARS-CoV-2 3CLpro	28.5827919
0.0761	C06	DMSO	Plate4	SARS-CoV-2 3CLpro	0.13456589
0.0685	C07	AZVIII-42	Plate4	SARS-CoV-2 3CLpro	-0.3704715

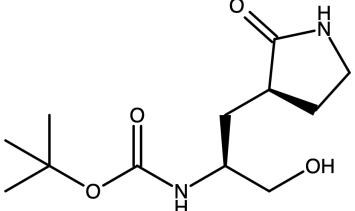
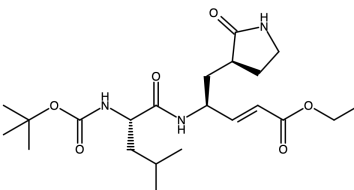
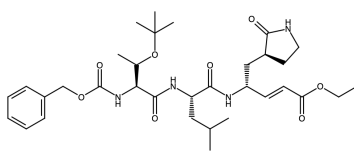
0.0781	C08	DMSO	Plate4	SARS-CoV-2 3CLpro	0.26747047
0.07245	C09	DMSO	Plate4	SARS-CoV-2 3CLpro	-0.107985
0.07745	C10	CC42746	Plate4	SARS-CoV-2 3CLpro	0.22427648
0.07475	C11	DMSO	Plate4	SARS-CoV-2 3CLpro	0.0448553
0.07445	D02	DMSO	Plate4	SARS-CoV-2 3CLpro	0.02491961
0.07965	D03	BTB07789	Plate4	SARS-CoV-2 3CLpro	0.37047153
0.41755	D04	GC376	Plate4	SARS-CoV-2 3CLpro	22.8247009
0.0346	D05	AZVIII-40A	Plate4	SARS-CoV-2 3CLpro	-2.6232042
0.04545	D06	BTB07420	Plate4	SARS-CoV-2 3CLpro	-1.9021968
0.06985	D07	DMSO	Plate4	SARS-CoV-2 3CLpro	-0.2807609
0.07115	D08	DMSO	Plate4	SARS-CoV-2 3CLpro	-0.194373
0.0744	D09	AZVIII-44E	Plate4	SARS-CoV-2 3CLpro	0.021597
0.0888	D10	DMSO	Plate4	SARS-CoV-2 3CLpro	0.97850999
0.0955	D11	MWP00710	Plate4	SARS-CoV-2 3CLpro	1.42374035
0.1017	E02	BTB07421	Plate4	SARS-CoV-2 3CLpro	1.83574456
0.09715	E03	DMSO	Plate4	SARS-CoV-2 3CLpro	1.53338663
0.0795	E04	MAC-30731	Plate4	SARS-CoV-2 3CLpro	0.36050368
0.08255	E05	DMSO	Plate4	SARS-CoV-2 3CLpro	0.56318317
0.1028	E06	NT 1-24	Plate4	SARS-CoV-2 3CLpro	1.90884208
0.0716	E07	DMSO	Plate4	SARS-CoV-2 3CLpro	-0.1644694
0.07325	E08	AZVIII-44D	Plate4	SARS-CoV-2 3CLpro	-0.0548231
0.0693	E09	DMSO	Plate4	SARS-CoV-2 3CLpro	-0.3173097
0.07195	E10	DMSO	Plate4	SARS-CoV-2 3CLpro	-0.1412111
0.0803	E11	DMSO	Plate4	SARS-CoV-2 3CLpro	0.41366552
0.0946	F02	DMSO	Plate4	SARS-CoV-2 3CLpro	1.36393329
0.09095	F03	AZVIII-44B	Plate4	SARS-CoV-2 3CLpro	1.12138242
0.07375	F04	DMSO	Plate4	SARS-CoV-2 3CLpro	-0.021597
0.0791	F05	NT 1-21	Plate4	SARS-CoV-2 3CLpro	0.33392277
0.0642	F06	DMSO	Plate4	SARS-CoV-2 3CLpro	-0.6562164
0.076	F07	SCR00533	Plate4	SARS-CoV-2 3CLpro	0.12792066
0.07345	F08	DMSO	Plate4	SARS-CoV-2 3CLpro	-0.0415327
0.05335	F09	Glecaprevir	Plate4	SARS-CoV-2 3CLpro	-1.3772237
0.0681	F10	SEW03089	Plate4	SARS-CoV-2 3CLpro	-0.3970524
0.07905	F11	DMSO	Plate4	SARS-CoV-2 3CLpro	0.33060015
0.0656	G02	Doravirine	Plate4	SARS-CoV-2 3CLpro	-0.5631832
0.0011	G03	Delanzomib	Plate4	SARS-CoV-2 3CLpro	-4.849356
0.0675	G04	Morroniside	Plate4	SARS-CoV-2 3CLpro	-0.4369238
0.04885	G05	Calycosin-7-O-beta-D-glucoside	Plate4	SARS-CoV-2 3CLpro	-1.6762591

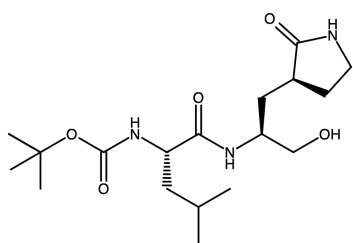
0.05495	G06	Glabridin	Plate4	SARS-CoV-2 3CLpro	-1.2709001
0.0358	G07	Licochalcone A	Plate4	SARS-CoV-2 3CLpro	-2.5434615
0.01645	G08	Velpatasvir	Plate4	SARS-CoV-2 3CLpro	-3.8293133
0.0393	G09	Telaprevir	Plate4	SARS-CoV-2 3CLpro	-2.3108784
0.0612	G10	Odanacatib	Plate4	SARS-CoV-2 3CLpro	-0.8555733
0.08295	G11	Darunavir	Plate4	SARS-CoV-2 3CLpro	0.58976409
0.0721	H02	Danoprevir	Plate4	SARS-CoV-2 3CLpro	-0.1312433
0.03045	H03	Nelfinavir Mesylate	Plate4	SARS-CoV-2 3CLpro	-2.8989812
0.00735	H04	Oprozomib	Plate4	SARS-CoV-2 3CLpro	-4.4340292
0.0658	H05	AEBSF hydrochloride	Plate4	SARS-CoV-2 3CLpro	-0.5498927
0.075	H06	Belnacasan	Plate4	SARS-CoV-2 3CLpro	0.06146837
0.0761	H07	Z-DEVD-FMK	Plate4	SARS-CoV-2 3CLpro	0.13456589
0.1242	H08	Z-FA-FMK	Plate4	SARS-CoV-2 3CLpro	3.33092112
0.0698	H09	Trovirdine	Plate4	SARS-CoV-2 3CLpro	-0.2840835
0.0076	H10	MG132	Plate4	SARS-CoV-2 3CLpro	-4.4174161
0.05275	H11	Cabotegravir	Plate4	SARS-CoV-2 3CLpro	-1.4170951

100

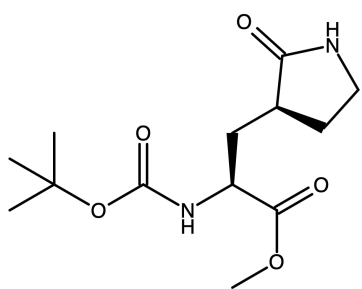
101

Supplementary Table 3. Structures of synthesized and structurally similar compounds for this study.

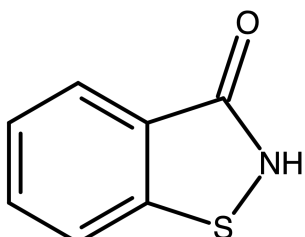
Compound	Structure
AZVIII-30	
AZVIII-33B	
AZVIII-34D	



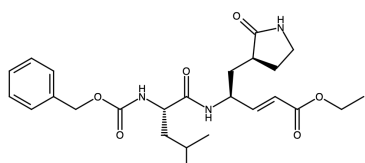
AZVIII-37A



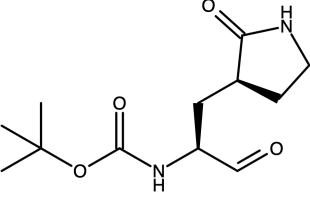
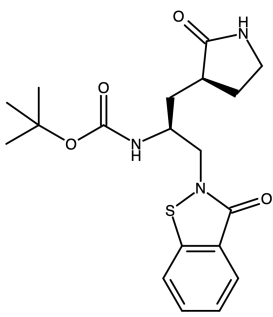
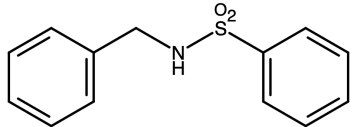
AZVIII-38

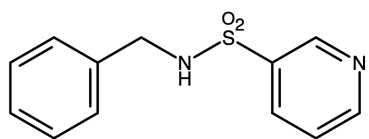


AZVIII-40A

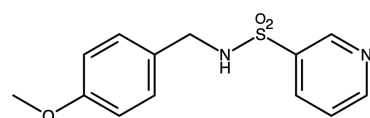


AZVIII-41A

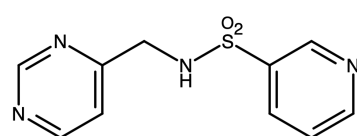
AZVIII-42	
AZVIII-43A	
AZVIII-44B	
AZVIII-44D	



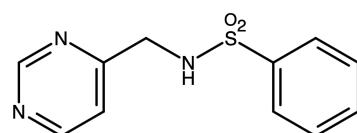
AZVIII-44E



AZVIII-44H



AZVIII-49C

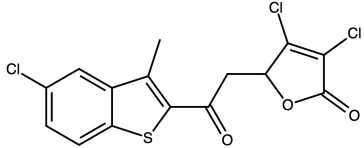
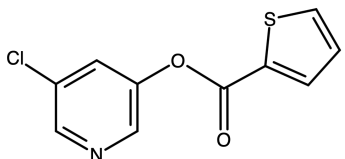
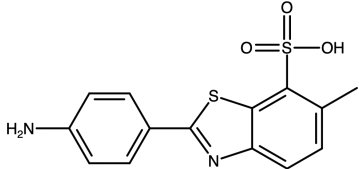
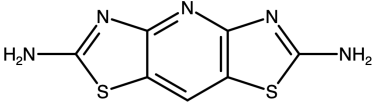


AZVIII-49F

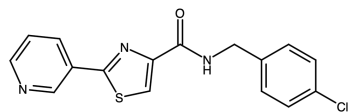
AZVIII-57D	
AZVIII-57G	
GC373	
BTB07404	

	<chem>O=S(=O)(c1ccc(Cl)ccn1)Oc2ccc(Cl)cc2</chem>
BTB07407	<chem>O=C(c1ccsc1)c2ccc(Cl)ccn2</chem>
BTB07408	<chem>O=C(c1ccc(Cl)ccn1)c2c(C)nn3ccccc23</chem>
BTB07417	<chem>O=[N+]([O-])c1ccc(Cl)cc(Oc2ccc(C(F)(F)F)cc2)c1</chem>
BTB07420	

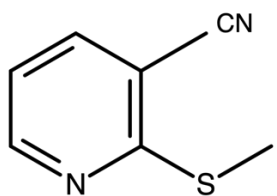
	<chem>O=[N+]([O-])c1ccc(Oc2cc(Cl)ccn2)cc1</chem>
BTB07421	<chem>CC(=O)Nc1ccc(Oc2cc(Cl)ccn2)cc1</chem>
BTB07789	<chem>CNCCc1cc(Oc2cc(Cl)ccn2)oc1</chem>
CC42746	<chem>CC1=Cc2ccccc2C(=O)Oc1cc(Cl)ccn1</chem>
GRL-0496	

	
MAC-30731	
	
MAC-5576	
	
MAC-8120	
	
MAC22272	

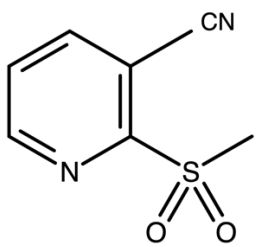
MWP00332	
MWP00333	
MWP00508	
MWP00709	



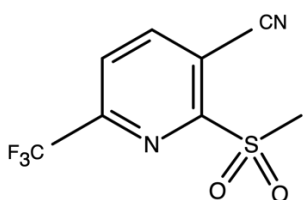
MWP00710



NT 1-21



NT 1-24



NT 1-32

	<chem>CN(CC(=O)c1cnc2ccccc12)Cc3ccncc3</chem>
SCR00533	<chem>CN(Cc1ccccc1)Cc2ncsc2Cc3ccccc3OC</chem>
SEW03089	<chem>CN(CC(=O)c1cnc2ccccc12)C2=CC=CC3=C2ONC3</chem>
SPB06591	<chem>CN(CC(=O)c1cnc2ccccc12)C2=CC=CC3=C2ONC3</chem>
SPB06593	<chem>CN(CC(=O)c1cnc2ccccc12)C2=CC=CC3=C2ONC3</chem>

	<chem>C(F)(F)c1ccc(NC(=O)CC2N3C=CNC3C(=O)OC2)cc1</chem>
SPB06613	<chem>Clc1ccc(C(=O)CN2C3C=CNC3C(=O)OC2)cc1</chem>
SPB06636	<chem>Clc1ccc(C(=O)NCC2N3C=CNC3C(=O)OC2)cc1</chem>
SPB08384	

103

104

105 **Supplementary Table 4. DNA sequences of proteases used in this study**

Protease	Genbank Accession	Sequence
Bat-CoV-HKU4 3CLpro	EF065505	atgagtggttgttaagatgtcagctcctagtggctgttagagaactgtattgtcaagttacatgtgggtcta tgacattgaatggcttggctgataacactgtatggtcctgcatttatgtgtccgcataact gacccaaattatgatgttttgttaattcaaaaaactaatcatatgtttttatgtcaaaaacacataggagctag gctaatctgcgttgtgtctcattctatggctgttgtactaaggtaactgtgtatgtcaatcttagtacacc agcatatacttttagtactgttaaaacctggccctcgtttagcgttttagctgttataatggcaagccacagggt tcittacagttaattacgcacaattctaccatcaaaggcagttccctgtggtgtgttagtggttacact gaaaatggaggtgtaatcaactgtttatgtcatcagatggattatcaatggtacacatactggtagttc ttttaggttgtatgtatggcttttgttaagataaaacacaccaggtaactaacagacaataactgcac tattaatgttagtagctggctctatgcaggcgttcttttttttttttttttttttttttttttttttttttt aattgttaacttataatgaatggcttgttagtaatcagttacagaaattgttaggcacacagtccattgtatgctt gctaccgaactgggtttctgtgaacaaatgtcgtctatccagagtctgcacatgcgttgtttagggtaaa actattctggccaggactactttggaggatgaggtaactcctgtatgttaatatgcaagtcatgggttgtaa tgcaattaa
Bat-CoV-HKU4 3CLpro C148A	EF065505	atgagtggttgttaagatgtcagctcctagtggctgttagagaactgtattgtcaagttacatgtgggtcta tgacattgaatggcttggctgataacactgtatggtcctgcatttatgtgtccgcataact gacccaaattatgatgttttgttaattcaaaaaactaatcatatgtttttatgtcaaaaacacataggagctag gctaatctgcgttgtgtctcattctatggctgttgtactaaggtaactgtgtatgtcaatcttagtacacc agcatatacttttagtactgttaaaacctggccctcgtttagcgttttagctgttataatggcaagccacagggt tcittacagttaattacgcacaattctaccatcaaaggcagttccctgtggtgttctGCCggtagtgtgttac actgaaaatggagggtgtaatcaactttttatgtcatcagatggattatcaatggtacacatactggtagt tcitttgcgttgtatgtatggcttttgttaagataaaacacaccaggtaacagacaataactg cactattaatgttagtagctggctctatgcacgcgttctaaatgggttagtggtttagggtaaaacccaccagg tggaaatgttaacttataatgaatggcttgttagtaatcagttacagaaattgttaggcacacagtccattgtat cctgcaccgaactgggtttctgtgaacaaatgtcgtctatccagagtctgcacatgcgttgtttagggtaa aaactattctggccaggactactttggaggatgaggtaactcctgtatgttaatatgcaagtcatgggttgt aatgcaggtaaa
Bat-CoV-HKU9 3CLpro	EF065513	atggccggccctgacacgtatggctcaccctcagggttagtagagccgtgcctgttaaagtaaaattatggtc catgactcttaatggtatatggtgataatttttataatgtcctaggcatgtttagtgcgtttagggatgagttagct aatcctgattaccctcggtgtctatgcacgcgtctaaatgtatgtttcacgtgtctcaaaatggcataatattcg gttataggccatactatggaaagggtcgctttaaaagctaacagtgtatgtgaataatcctaaaacacccgttt tcatttacgggtgagttacgggtcaagctatgtatgggttgcacgttgtatgtatggttaccaactgggttat gtgcacttacgggtcaatggtactatggatggcatcattttatgtggctctgtggtagtgcctgggttgc atggcaaaaggtaatttttacaccaggcttgaaattaccatggtactctataactggtagcatttttc tgggtctttatggccatttgcaggacaagaaggcaatgcgcataaggcgttgcattttatgcgttatgttac gttttagcatggcatttgcacgtgttagtttacaccaggcatggtagtttgatgttagtatttgc atggcaaaaggtaatttttgcatttgcaggatgcacacccgttgcatttttgcatttttgcatttttc actattatggccctgtttagggatgaggatgaggatgcataccgtatgtatggccgtcaaatgttaggtt tgcataaa
Bat-CoV-HKU9 3CLpro C144A	EF065513	atggccggccctgacacgtatggctcaccctcagggttagtagagccgtgcctgttaaagtaaaattatggtc catgactcttaatggtatatggtgataatttttataatgtcctaggcatgtttagtgcgtttagggatgagttagct aatcctgattaccctcggtgtctatgcacgcgtctaaatgtatgtttcacgtgtctcaaaatggcataatattcg gttataggccatactatggaaagggtcgctttaaaagctaacagtgtatgtgaataatcctaaaacacccgttt tcatttacgggtgagttacgggtcaagctatgtatgggttgcacgttgtatgtatggttaccaactgggttat gtgcacttacgggtcaatggtactatggatggcatcattttatgtggctctGCCggtagtgcctgggttgc gtatggcaaaaggtaatttttgcatttgcaggatgcacacccgttgcatttttgcatttttgcatttttc tgcatttttgcatttttgcatttttgcatttttgcatttttgcatttttgcatttttgcatttttgcatttttc actattatggccctgtttagggatgaggatgaggatgcataccgtatgtatggccgtcaaatgttaggtt tgcataaa

		acgtactatactgtttatggctctgtgtacgaattcacgcctactgaagtataaggcaaatgtatggtta aatcttcagtaa
HCoV- 229E 3CLpro	AF304460	atggctggttgcgcaaaatggcacaaccatctggcttggagaaaatgtgtccgtgtctatggaaa cactgttgtgaatgggttgccgtggatattgtttatgcacgttatcgcatctaaccacacttcgc tatagattatgatcacgaatatagtagttatgcgggtgcataatttctataatctgtacagcatttgggttg taggtctactatgcacggagaactctaaaattaagggttacagactaactgcacacactagacattct tttagaacactaaaatcggtgaagggttacatctgcacatgtatgggtgtcaagggtttttgggt aacatgagaactaattggactatccgtggcatttataatggcgtgtggccccgtacaatcttaaaa atggcagggtaattttatgcacaaattgaactcggaaatgttagccatgttagttctagcttgatg gtttatgtatgggtttgaagaccaactatctcaagtgaaatgcacacaggatgttaacagttatg gggtcattttatgcacatgtatgggtgtggcttaaaggtaaaaaattgttggagcatt ataatgagtggcacaggctaattgttacagactatgaatggtaagacgcctttccattctgctctaa actgggtctgtgtggaaagattactcatgtattcaagttgaataatggcttgggtaaacaaaatttgg ttattctagtctcaatgttagttcagttataatgaagttgtcaaaacaaaatgttgggttaacctgcaataa
HCoV- 229E 3CLpro C144A	AF304460	atggctggttgcgcaaaatggcacaaccatctggcttggagaaaatgtgtccgtgtctatggaaa cactgttgtgaatgggttgccgtggatattgtttatgcacgttatcgcatctaaccacacttcgc tatagattatgatcacgaatatagtagttatgcgggtgcataatttctataatctgtacagcatttgggttg taggtctactatgcacggagaactctaaaattaagggttacagactaactgcacacactagacattct tttagaacactaaaatcggtgaagggttacatctgcacatgtatgggtgtcaagggtttttgggt aacatgagaactaattggactatccgtggcatttataatggcgcGCCgggtccctggctacaatcttaa aaatggcagggtaattttatgcacaaattgaactcggaaatgttagccatgttagttctagcttg tgggttattgtatgggtttgaagaccaacctaattcaagtgaaatctgcaaccaggatgttaacagttat gtgggtcattttatgcacatgtatgggtcacatgggtgtcaaggtaaaaaattgttggagca ttataatgagtggcacaggctaattgttacagactatgaatggtaagacgcctttccattctgctctaa aactgggtctgtgtggaaagattactcatgtattcaagttgaataatggcttgggtaaacaaaatttgg gttattctagtctcaatgttagttcagttataatgaagttgtcaaaacaaaatgttgggttaacctgcaataa
HCoV- HKU1 3CLpro	AY597011	atgcaggattgtaaagatgttatccctacgtcaaaaatgaaccctgtattgttagttactatggtagtatg actttaatggttatggtagatgacaaagttattgtccctgtatgtttatctctataatgaac ctgattattctgcctattatgttagatgtacttagttactataatgtctggccggatgagtttaacagttgt gtttaccagatgcaggctgtcaactgtttacagtcattttacaaaatcttacactccaaaatacttt gtgtgttaaacctggtaacattttactgtttacatgcgtataatggccgaccacaaggggcatttcatt atgcgttagttataactattaaagggtctttgtgtggcatgtggatctgtgttatgttataacagggtata gtgttaagtttatgtatgcacattagactgttagttactgtgtccactgtgtttactgtgttatttt tggccatataagatgtcaagtgttagatgtccaggtaaggactacgtccaaactgttaatgttattgt gctctatgcagctataacttaataattgtctgggttacaaaatgtatgtttctatgttaagatttaatgttgg ctatgacaaaatgttttagccaagtaaaacgcagatctgttttagatgttggctcaatgcacagggtttctatt gaaactttatggctcttataagcgtctatataatggattcaaggcgtcaaaactacttagaagttgtacttt agatgaattggcacccctgcacgtttatcaacaatgggtgttaattgtcaataa
HCoV- HKU1 3CLpro C145A	AY597011	atgcaggattgtaaagatgttatccctacgtcaaaaatgaaccctgtattgttagttactatggtagtatg actttaatggttatggtagatgacaaagttattgtccctgtatgtttatctctataatgaac ctgattattctgcctattatgttagatgtacttagttactataatgtctggccggatgagtttaacagttgt gtttaccagatgcaggctgtcaactgtttacagtcattttacaaaatcttacactccaaaatacttt gtgtgttaaacctggtaacattttactgttagatgcgtataatggccgaccacaaggggcatttcatt atgcgttagttataactattaaagggtctttgtgtggcaGCCggatgtgtgttatgttataacagggtata taggttaagtttatgtatgcacattagactgttagttactgtgtccactgtgtttactgtgttatttt tatggccatataagatgtcaagtgttagatgtccaggtaaggactacgtccaaactgttaatgttattgt ggctctatgcagctataacttaataattgtctgggttacaaaatgtatgtttctatgttaagatttaatgttgg gctatgacaaaatgttttagccaagtaaaacgcagatctgttttagatgttggctcaatgcacagggtttctat tgaaactttatggctcttataagcgtctatataatggattcaaggcgtcaaaactacttagaagttgtacttt agatgaattggcacccctgcacgtttatcaacaatgggtgttaattgtcaataa
HCoV- NL63 3CLpro	AY567487	atgtctggcttaagaagatggcacaaccatctgggtgttagatgtgtccgtgtttatggtagta ctgtgtttatggtaggtacactgtttactgtccatgcacatgtcatagcaccatcaaccactgttct attgattatgtatcatgtatgtactatgcgtttgcataatttcagttgtcttataatgtgtcttggggatgttt

		aatattttggcatggcttatgcagcaattattagtgttaaagagagtagtggctgaaa gtactactatcagttatgtgattataataagtggcagggtataatggttacatcattgtaa attactaaattaagtgtataacaggagtagatgtttgaaactccttcgtactattatggaaa tgggttagtgaccctatttggacaataataatttgaggatgaaatgacaccgaatctgttt aatacttgggttagttacaataa
IBV 3CLpro C143A	KX236013	atggctggtttaagaaacttagtgtccctagtagtgctgtgagaagtgcattgttagtgtcttatagaggca gtaatcttaatggattgtgggggattccatctactgtccacgacatgtttaggttaagttagtgttt atggagtgtatgtacttagcctgctaataatcatgaaatttgagggttagtactcataatggttacttgta caggaggcgtaaagggtgcattactgatttcacagactgcagtagccaatgctgatcaccgaagtaaa attttggaaagcaaattgtgttagttcacaatagctgtcttatgtgttagtactttagacttacccc gttactatcgcttaatgaaactattagagcatgttttgctggagcaGCCgttcagtaggtttatata gaaaagggttagttaattttactacatgcaccatctagagtaccataatgcattacacacaggaaactgacc taatgggttagttatgtgttagtataatgaaagagggtgcagaaaatgtcaacccgataaattgtacta ataatatttggcatggcttatgcagcaattattagtgtttaaagagagtagtttcaacacaaaatggctga aagtactactatcagttatgtgattataataatggcagggtataatggttacatcattgtaa gcttactaaattaagtgtataacaggagtagatgtttaaactccttcgtactattatggtaaaaatgtca caatggggtagtgaccctatttggacaataataatttgaggatgaaatgacaccgaatctgttt taggtggtagttacaataa
MERS- CoV 3CLpro	JX869059	atgagcggttggtaaaatgtcacatcccagtggagatgttagggctgttatggttcaggttacctgcggtag catgactctaattgtcttgcgtgacaacacagtctgtgccacacacgttaatgtcccggtgaccag ttgtctgatcctaattatgtatgcctgtgattttatgactaataatcatagttcagtgtgaaaaacacattggcgt ccagcaaacttgcgtgtttgtcatgcatcaaggcacttttgaagttactgtcatgtctataatggc agcactccagccatactttacaacagtgaaacacctggcgcagcatttagtggtagcatgtctataatggc gtccgactggatattcactgtgttagtgcgttcaatgcgcctaactacacaatggttccctgtgtgttt agttgggttacccaaggaggtagtggtagtgcataatttttgcattcatgcatcaatggaaactgtcaatggtac acataccggttcagttgtactatgtatggctttatggataaaacaatgtcaccaagtgcaccaacttcagtt agacaaatactgcgtttaatgttagtgcgttgcattaccaatgtatgggtccaccaattactgttgcactcaat ccgttgcacatgttagtgcgtcaaaacaggcgtgttgcattgaacagctgtttatgcgtatccaacaactgtataact gggtccaggaaaagcaaattcctggcgttacccatgttggaaagatgaattcacacctgaggatgttaatatg cagattatgggtgtttatgcgttaaa
MERS- CoV 3CLpro C148A	JX869059	atgagcggttggtaaaatgtcacatcccagtggagatgttagggctgttatggttcaggttacctgcggtag catgactctaattgtcttgcgtgacaacacacagtctgtgccacacacgttaatgtcccggtgaccag ttgtctgatcctaattatgtatgcctgtgattttatgactaataatcatagttcagtgtgaaaaacacattggcgt ccagcaaacttgcgtgtttgtcatgcatcaaggcacttttgaagttactgttagcatgtctataatggc agcactccagccatactttacaacagtgaaacacctggcgcagcatttagtggtagcatgtctataatggc gtccgactggatattcactgtgttagtgcgttcaatgcgcctaactacacaatggttccctgtgtgttctGCCg gtagtgtgggttacccaaggaggtagtggtagtgcataattttgcattcatgcatcaatggaaactgtcaatggta cataccggttcagcattgtgtactatgtatggctttatggataaaacaatgtcaccaagtgcaccaacttcagtt cagacaataactgcgtttaatgttagtgcgttgcattaccaatgtatgggtccaccaattactgtatgggttt aacctaatactgcactgtgtttatggataatgggtcttgccaaaccaattactgtatgggtccaccaactgtataact tccgttgcacatgttagtgcgtcaaaacaggcgtgttgcattgaacagctgtttatgcgtatccaacaactgtataact gggtccaggaaaagcaaattcctggcgttacccatgttggaaagatgaattcacacctgaggatgttaatatg cagattatgggtgtttatgcgttaaa
PEDV 3CLpro	MH243316	atggctggctgcgttaagatggcacaaccatctgggtgttagaagtgtatagttcgtttgttatggtaata tggctctaattggctatggctggtagacactgttatctggccacgcgttatagcgttactactatcact atagattatgactatgcctttgtttacccctccacaacttctccatttcgttgcataatggttccatgttt gggttaaccatgcgggtgtttgcgttgcagataaaggtaatcaaacaatgtccacacgcctaagtgacacc tatgcacagttagaccgggtgaatctttatatctggcgttgcataatggttccatgttt taacatgcgtctaaattacactattagaggctgttgcattatggcgttgcgttgcacccgttataacattaac aatggtagccgttagtttgcattaccaggactgttgcactgtgtttgcgttgcacttagt gtttatgtatgggtttatggaccaacctactgttgcgttgcactgtgtttacagagaatgt tggcattttatgcgttgcactcattatggtttgcacccgttgcgttgcacttagtcttctaggattgttagacagggtt

117 carboxylic ester suffering from hydrolysis has been reported [2]. Thus, the covalent complex formed by
118 MAC-5576 could be reversed. Furthermore, benzothiophene is less electron-donating than thiophene,
119 suggesting a less stable cysteine adduct for BTB07408 than MAC-5576 [3]. Toward that end, triazole has
120 been reported to be an inductively electron-withdrawing group, hence BTB07417's irreversible inhibition is
121 most prone for interruption due to hydrolysis [4].

122
123 On the other hand, literature has shown that indole is electron-donating [5]. Therefore, GRL-0496 would
124 benefit from its electron-donating indole substituent to form a stable thioester bond with the catalytic cysteine
125 residue. In contrast, MAC-5576, BTB07408, and BTB07417 might undergo hydrolysis in the cell.

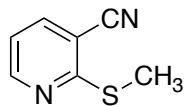
126
127 To corroborate this hypothesis, Verschueren et al. discussed a potential hydrolysis of the ester bond in the
128 compound itself or the thioester bond with the active-site cysteine that occur in a benzyloxy inhibitor, XP-
129 27, for SARS-CoV [1]. Conversely, the hydrolysis could be avoided with an electron-donating group to
130 decrease the electrophilicity of the carbonyl carbon and stabilize the ester or thioester bond. In such effort
131 the dimethylaminobenzoyloxy compound XP-59 was synthesized. Its SARS-CoV adduct is more stable, and
132 potent enzyme inhibition (IC_{50} : 0.1 μ M) was confirmed.

133
134 **Supplementary Materials and Methods**

135 **Chemical Synthesis**

136 All other compounds used in the study were synthesized and quality checked according to the following
137 protocols.

138

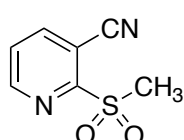


140 2-(methylthio)nicotinonitrile (xx-1) The title compound was prepared according to a published procedure;
141 spectral data are in agreement with literature values [6].

142 ^1H NMR (500 MHz, CDCl_3) δ 8.60 (dd, $J = 5.0, 1.8$ Hz, 1H), 7.79 (dd, $J = 7.7, 1.8$ Hz, 1H), 7.07 (dd, $J = 7.7,$
143 4.9 Hz, 1H), 2.64 (s, 3H).

144 ^{13}C NMR (126 MHz, CDCl_3) δ 163.7, 152.2, 140.6, 118.4, 115.7, 107.5, 13.4.

145 HRMS High accuracy (ASAP): Calculated for $\text{C}_7\text{H}_6\text{N}_2\text{S} (\text{M}+\text{H})^+$: 151.0330; found: 151.0327.



148 2-(methylsulfonyl)nicotinonitrile (xx-2) The title compound was prepared from xx-1 according to a modified
149 procedure from the literature [7].

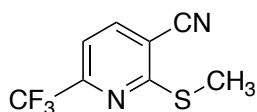
150 Pyridine xx-1 (87 mg, 0.58 mmol, 1 equiv) was weighed into 50 mL round bottom flask equipped with a stir
151 bar. The solid was dissolved in 10 mL of anhydrous MeOH, followed by portion-wise (usually 3 portions)
152 additions of mCPBA (500 mg, 2.9 mmol, 5 equiv). Substrate conversion was monitored via TLC analysis (70%
153 EtOAc:Hex to 100% EtOAc), with up to an additional 5 equiv of mCPBA added if necessary. Upon complete
154 conversion of starting material, the reaction was quenched with 20 mL of saturated aqueous NaHCO₃, diluted
155 with an additional 20 mL of DCM. The layers were separated and the organic layer was further washed (2x)
156 with 10 mL of saturated aqueous NaHCO₃. The organic layer was then dried *in vacuo* and purified via silica
157 gel column chromatography (100% EtOAc to 5% MeOH:EtOAc) to yield 51 mg (48% yield) of the desired
158 sulfone as a white solid.

159 ¹H NMR (400 MHz, CDCl₃) δ 8.86 (dd, *J* = 4.8, 1.6 Hz, 1H), 8.26 (dd, *J* = 7.9, 1.6 Hz, 1H), 7.70 (dd, *J* = 7.9,
160 4.8 Hz, 1H), 3.39 (s, 3H).

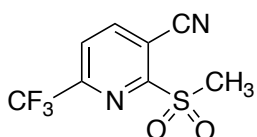
161 ¹³C NMR (101 MHz, CDCl₃) δ 159.8, 151.8, 143.8, 126.8, 113.2, 107.4, 40.1.

162 HRMS High accuracy (ASAP): Calculated for C₇H₆N₂O₂S (M+H)⁺: 183.0228; found: 183.0223.

163



165 2-(methylthio)-6-(trifluoromethyl)nicotinonitrile (xx-3) The title compound was prepared following the published
166 procedure, the product (yellow solid) was carried towards the synthesis of xx-4 without further purification [6].
167



169 2-(methylsulfonyl)-6-(trifluoromethyl)nicotinonitrile (xx-4) The title compound was prepared from xx-3
170 according to a modified procedure from the literature [7].

171 Pyridine xx-2 (105 mg, 0.50 mmol, 1 equiv) was weighed into 50 mL round bottom flask equipped with a stir
172 bar. The solid was dissolved in 10 mL of anhydrous MeOH, followed by portion-wise (usually 3 portions)
173 additions of mCPBA (0.86 mg, 5 mmol, 10 equiv). Substrate conversion was monitored via TLC analysis (40%
174 EtOAc:Hex to 60% EtOAc). Upon complete conversion of starting material, the reaction was quenched with
175 20 mL of saturated aqueous NaHCO₃, diluted with an additional 20 mL of DCM. The layers were separated
176 and the organic layer was further washed (2x) with 10 mL of saturated aqueous NaHCO₃. The organic layer
177 was then dried *in vacuo* and purified via silica gel column chromatography (40% to 80% EtOAc:Hex) to yield
178 38 mg (30% yield) of the desired sulfone as a white solid.

179 ¹H NMR (400 MHz, CDCl₃) δ 8.49 (dd, *J* = 8.1, 0.7 Hz, 1H), 8.06 (d, *J* = 8.1 Hz, 1H).

180 ^{13}C NMR (101 MHz, CDCl_3) δ 160.4, 149.7 (q, $J = 37.6$ Hz), 146.0, 123.7 (q, $J = 2.3$ Hz), 120.0 (q, $J = 275.5$ Hz), 112.1, 109.7, 39.7.

181 ^{19}F NMR (376 MHz, CDCl_3) δ -68.28.

182 HRMS High accuracy (ASAP): Calculated for $\text{C}_8\text{H}_5\text{F}_3\text{N}_2\text{O}_2\text{S} (\text{M}+\text{H})^+$: 251.0102; found: 251.0104.

184

185 Compound 11a was synthesized according to the specified protocol in Dai. et al. [8]. Compound 11a was
186 confirmed by LCMS with $m/z = 453$ ($\text{M}+1$) and 451 ($\text{M}-1$).

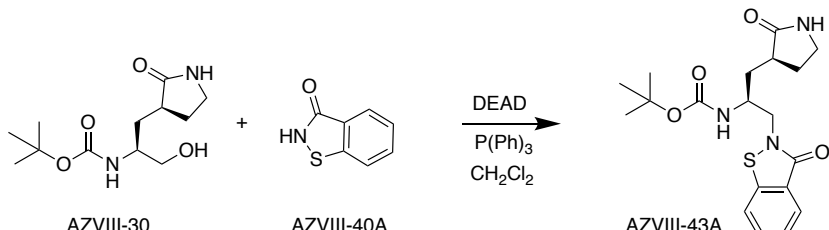
187

188 Compound 4 was synthesized according to the procedure described in Yang et al. [9]. AZVIII-34D was
189 formed as a byproduct (15%) in the synthesis of Compound 4 and was isolated by RP HPLC. ^1H NMR (400
190 MHz, CDCl_3) 7.88 (s, 1H), 7.44-7.34 (m, 5H), 6.80 (d, 1H, $J = 15.4$ Hz), 6.69 (s, 1H), 6.16-5.87 (m, 2H), 5.12
191 (s, 2H), 4.76 (s, 1H), 4.42 (s, 1H), 4.31-3.99 (m, 4H), 3.39 (s, 2H), 2.40-1.45 (m, 8H), 1.29-1.20 (m, 12H),
192 1.13-1.02 (m, 3H), 1.00 – 0.89 (m, 6H). MS $\text{M}+\text{H} = 631$.

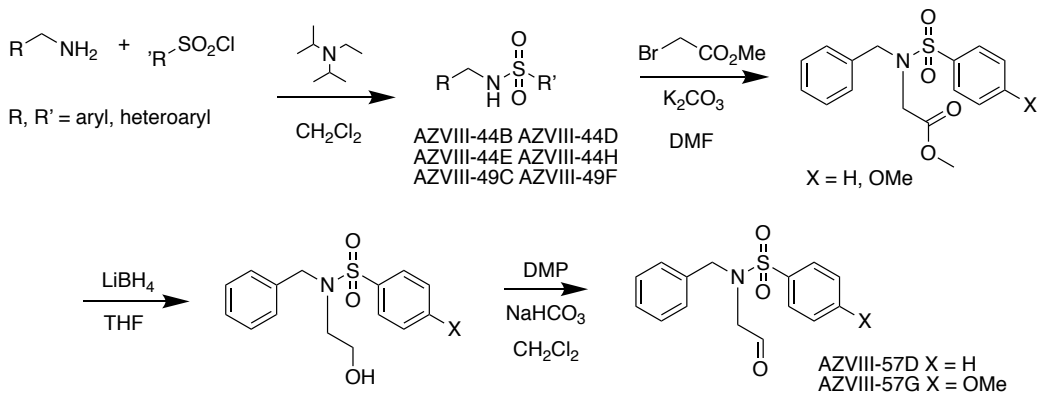
193 AZVIII-38, AZVIII-30, and AZVIII-42 were synthesized according the procedures described in Mou et al. [10].
194 AZVIII-37A was synthesized as described in Prior et al. [11]. AZVIII-33B was synthesized according to the
195 method described in Amblard et al. [12].

196 AZVIII-41A was synthesized according to the procedure described for synthesizing AZVIII-33B in Amblard et
197 al. and substituting Z-Leu-OH for BOC-Leu-OH [12]. ^1H NMR (400 MHz, CDCl_3) 7.77 (s, 1H), 7.41-7.27 (m,
198 5H), 6.80 (dd, 1H, $J = 5.5, 15.6$ Hz), 5.98-5.84 (m, 2H), 5.15-5.03 (m, 2H), 4.55 (bd s, 1H), 4.27 (bd s, 1H),
199 4.23-4.07 (m, 3H), 3.38-3.23 (m, 2H), 2.56–1.40 (m, 8H), 1.33 – 1.20 (m, 3H), 0.95 (s, 6H). MS $\text{M}+\text{H} = 474$.

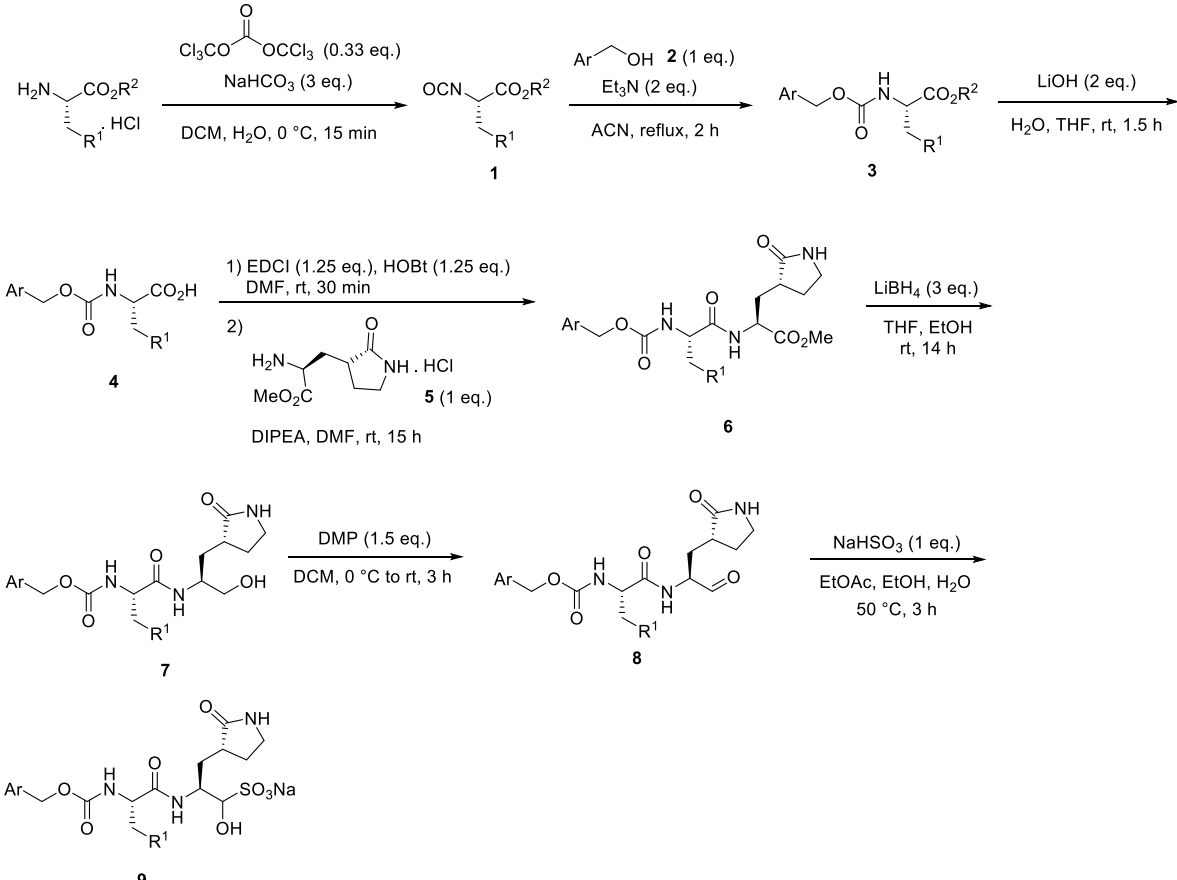
200 AZVII-43A was synthesized by treatment of a dichloromethane solution of AZVIII-30 and AZVIII-40A with
201 triphenyl phosphine and diethyl azodicarboxylate. ^1H NMR (400 MHz, CDCl_3) 7.91 (d, 1H, $J = 8.0$), 7.76 (d,
202 1H, $J = 8.0$), 7.55-7.34 (m, 2H), 6.16 (bd s, 1H), 5.29 (bd s, 1H), 4.73-4.39 (m, 2H), 4.35-3.96 (m, 1H), 3.58-
203 3.16 (m, 2H), 3.79-3.43 (m, 2H), 3.39-3.91 (m, 1H), 1.98-1.77 (m, 1H), 1.73-1.57 (m, 1H), 1.42 (s, 9H). MS
204 $\text{M}+\text{H} = 392$.



211 dimethylformamide to give the corresponding ester which was reduced to the corresponding alcohol by
 212 treatment with lithium borohydride in tetrahydrofuran. The alcohol was then treated with 1,1,1-
 213 tris(acetoxy)-1,1-dihydro-1,2-benziodoxol-3-(1*H*)-one and sodium bicarbonate in dichloromethane to give
 214 to the corresponding aldehyde AZVIII-57D. AZVIII-57G was synthesized from *N*-benzyl-4-
 215 methoxybenzenesulfonamide according to the procedure used to synthesize AZVIII-57D.



216
 217 GC373 was synthesized from GC376 by converting the bisulfite group to an aldehyde group by treatment
 218 with aqueous sodium bicarbonate. To a solution of 5.31 mg of GC376 in 200 μL H_2O , 2 μL of saturated
 219 NaHCO_3 was added. The cloudy mixture was extracted with CH_2Cl_2 , dried over Na_2SO_4 , and concentrated in
 220 vacuo to give GC373 as a colorless oil (4.0 mg).
 221
 222 SL-4-241 was synthesized according to the following general procedure:



223

224 Glutamine surrogate 5 was synthesized according to previously described procedure and its spectral data
225 were in agreement with the published values [13].

226 General procedure for synthesis of carbamate 3

227 Following the published procedure, triphosgene (0.33 equiv.) was added into a cooled (0 °C) vigorously
228 stirred mixture of methyl or ethyl ester of amino acid hydrochloride (2.5 mmol, 1 equiv.) in NaHCO₃ (10 mL,
229 sat. aq.sol.) and DCM (10 mL) [14]. After stirring at 0 °C for 15 min, the phases were separated and
230 aqueous phase was extracted with DCM (3×). The combined organic layers were dried over MgSO₄.
231 Filtration and evaporation of solvents gave isocyanate 1, which was used in the next step without any further
232 purification.

233 Following the published procedure, isocyanate 1, alcohol 2 (1 equiv.) and Et₃N (2 equiv.) were refluxed in
234 MeCN (10 mL) for 2 h [15]. The reaction mixture was then concentrated under reduced pressure, diluted by
235 EtOAc, washed with HCl (5%, 1×) and brine (1×), dried over Na₂SO₄, filtered and concentrated under
236 reduced pressure. Column chromatography of the residue on silica gel (hexane/EtOAc) yielded carbamate
237 3.

238 General procedure for synthesis of acid 4

239 Following the published procedure, carbamate 3 (2 mmol, 1 equiv.) and LiOH (2 equiv.) were stirred in a
240 mixture of H₂O/THF (10 mL, 3/2) for 16 h at rt [15]. Reaction mixture was then concentrated under reduced

241 pressure, diluted by H₂O, acidified by HCl (5%) to pH 2 and extracted with EtOAc (3×). The combined
242 organic layers were then dried over Na₂SO₄. Filtration and evaporation of solvents gave acid 4, which was
243 used in the next step without any further purification.

244 General procedure for synthesis of ester 6

245 Following the published procedure, acid 4 (0.7 mmol, 1 equiv.) and HOEt (1.25 equiv.) were added to the
246 pre-stirred (30 min) solution of EDCI.HCl (1.25 equiv.) and DIPEA (1.4 equiv.) in DMF (8 mL) and the
247 reaction mixture was stirred for 30 min at rt [15]. In a separate flask, a cooled (0°C) solution of glutamine
248 surrogate 5 (1 equiv.) in DMF (2 mL) was treated with DIPEA (4 equiv.). After stirring for 30 min at 0 °C, the
249 glutamine surrogate 5 solution was transferred to the mixture with acid 4 and the resulting reaction mixture
250 was stirred at rt for 15 h. The majority of solvents was evaporated under reduced pressure. The residue was
251 then diluted by EtOAc, washed with citric acid (10% aq. sol., 3×), NaHCO₃ (sat. aq. sol., 1×) and brine (1×),
252 dried over Na₂SO₄, filtered and concentrated under reduced pressure. Column chromatography of the
253 residue on silica gel (DCM/MeOH) yielded ester 6.

254 General procedure for synthesis of alcohol 7

255 Following the published procedure, ester 4 (0.4 mmol, 1 equiv.) and LiBH₄ (4 equiv.) were stirred in dry THF
256 (4 mL) and absolute EtOH (1 mL) under Ar atmosphere for 12 h [15]. The reaction was quenched by
257 addition of H₂O and acidified by HCl (5%) to pH 2. The solvent was removed under reduced pressure and
258 the residue was diluted by EtOAc, washed with brine (1×), dried over Na₂SO₄, filtered and evaporated under
259 reduced pressure. Column chromatography of the residue on silica gel (DCM/MeOH) yielded alcohol 7.

260 General procedure for synthesis of aldehyde 8

261 Following the published procedure, DMP (1.5 equiv.) was added to a cooled (0 °C) solution of alcohol 7 (0.3
262 mmol, 1 equiv.) in dry DCM (5 mL) under Ar atmosphere [15]. The mixture was stirred at 0 °C for 5 min and
263 then at rt for 3 h. Reaction was quenched by addition of a mixture of Na₂S₂O₃ (5 mL, 10% aq. sol.) and
264 NaHCO₃ (5 mL, sat. aq. sol.). After 5 min stirring at rt, the phases were separated and the aqueous phase
265 was extracted with DCM (3×). The combined organic layers were then washed with brine (2×), dried over
266 Na₂SO₄ and concentrated under reduced pressure. Column chromatography of the residue on silica gel
267 (DCM/MeOH) yielded aldehyde 8.

268 General procedure for synthesis of bisulfite adduct 9

269 Following the published procedure, aldehyde 8 (0.1 mmol, 1 equiv.) and NaHSO₃ (1 equiv.) were stirred in a
270 mixture of EtOAc (0.5 mL), EtOH (0.25 mL) and H₂O (0.1 mL) at 50 °C for 3 h [15]. The solvents were then
271 evaporated and the residue was washed with EtOAc (3×). The solid was then dissolved in EtOH, filtered
272 through cotton and dried under reduced pressure. Washing of the solid residue with Et₂O (2×) and mixture of
273 Et₂O/EtOAc (2/1, 1×) yielded bisulfite adduct 9.

274

275

276

277

278

279

280 SL-4-241: Yield: 10% in 7 steps. White solid.

281 ^1H NMR (400 MHz, CD₃OD) δ 7.43 – 7.28 (m, 5H), 5.20 – 5.07 (m, 2H), 4.55 – 4.47 (m, 1H), 4.28 – 4.17 (m, 1H), 4.04 – 3.94 (m, 1H), 3.36 – 3.16 (m, 2H), 2.51 – 2.39 (m, 1H), 2.36 – 2.27 (m, 1H), 2.09 – 1.97 (m 1H), 1.88 – 1.13 (m, 13H), 1.08 – 0.89 (m, 2H).284 IR (CD₃OD, cm⁻¹) ν 3385, 2924, 2489, 2239, 2073, 1673, 1423, 1345, 1194, 1153, 1117, 971, 901.285 LRMS (ESI) m/z [C₂₄H₃₄N₃O₈S]⁺ ([M]⁺) calculated 524.2, found 524.3.

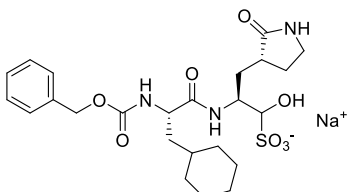
286

287 **Supplemental References**

288

289 1. Verschueren KHG, Pumpor K, Anemüller S, Chen S, Mesters JR, Hilgenfeld R. 2008. A Structural View of
290 the Inactivation of the SARS Coronavirus Main Proteinase by Benzotriazole Esters. Chem. Biol. 15, 597–
291 606.292 2. Bastide J, Badon R, Cambon J, Vega D. 1994. Transformation rates of ortho-substituted thiophene and
293 benzene carboxylic esters: Application to thifensulfuron-methyl and metsulfuron-methyl herbicides. Pestic.
294 Sci. 40, 293–297.295 3. Cativiela C, Garcia JI. 1990. Electronic effects of heterocyclic substituents. Spectroscopical and
296 theoretical (AM1) study in a series of heterocyclic carboxaldehydes. Can. J. Chem. 68, 1477–1481.297 4. Creary X, Chormanski K, Peirats G, Renneburg C. 2017. Electronic Properties of Triazoles. Experimental
298 and Computational Determination of Carbocation and Radical-Stabilizing Properties. J. Org. Chem. 82,
299 5720–5730.300 5. Szent-Györgyi A, Isenberg I. 1960. On the electron donating properties of indoles. Proc. Natl. Acad. Sci.
301 U. S. A. 46, 1334–1336.302 6. Metzger A, Melzig L, Despotopoulou C, Knochel P. 2009. Pd-Catalyzed Cross-Coupling of Functionalized
303 Organozinc Reagents with Thiomethyl-Substituted Heterocycles. Org. Lett. 11, 4228–4231.304 7. Zambaldo C, Vinogradova EV, Qi X, Iaconelli J, Suciu RM, Koh M, Senkane K, Chadwick SR, Sanchez
305 BB, Chen JS, Chatterjee AK, Liu P, Schultz PG, Cravatt BF, Bollong MJ. 2020. 2-Sulfonylpyridines as
306 Tunable, Cysteine-Reactive Electrophiles. J. Am. Chem. Soc. 142, 8972–8979.

307

308 8. Dai W, Zhang B, Jiang X, Su H, Li J, Zhao Y, Xie X, Jin Z, Peng J, Liu F, Li C, Li Y, Bai F, Wang H,
309 Cheng X, Cen X, Hu S, Yang X, Wang J, Liu X, Xiao G, Jiang H, Rao Z, Zhang L, Xu Y, Yang H, Liu H.
310 2020. Structure-based design of antiviral drug candidates targeting the SARS-CoV-2 main protease.
311 Science 368, 1331–1335

- 312 9. Vuong W, Khan MB, Fischer C, Arutyunova E, Lamer T, Shields J, Saffran HA, McKay RT, van Belkum
313 MJ, Joyce MA, Young HS, Tyrrell DL, Vederas JC, Lemeieux MJ. 2020. Feline coronavirus drug inhibits the
314 main protease of SARS-CoV-2 and blocks virus replication. *Nat. Commun.* 11, 4282.
- 315 10. Mou K, Xu B, Ma C, Yang X, Zou X, Lü Y, Xu P. 2008. Novel CADD-based peptidyl vinyl ester
316 derivatives as potential proteasome inhibitors. *Bioorg. Med. Chem. Lett.* 18, 2198–2202.
- 317 11. Prior AM, Kim Y, Weerasekara S, Moroze M, Alliston KR, Uy RA, Groutas WC, Chang KO, Hua DH.
318 Design, synthesis, and bioevaluation of viral 3C and 3C-like protease inhibitors. 2013. *Bioorg. Med. Chem.*
319 Lett. 23, 6317–6320.
- 320 12. Amblard F, Zhou S, Liu P, Yoon J, Cox B, Muzzarelli K, Kuiper BD, Kovari LC, Schinazi RF. 2018.
321 Synthesis and antiviral evaluation of novel peptidomimetics as norovirus protease inhibitors. *Bioorg. Med.*
322 *Chem. Lett.* 28, 2165–2170.
- 323 13. Zhai Y, Zhao X, Cui Z, Wang M, Wang Y, Li L, Sun Q, Yang X, Zeng D, Liu Y, Sun Y, Lou Z, Shang L,
324 Yin Z. 2015. Cyanohydrin as an Anchoring Group for Potent and Selective Inhibitors of Enterovirus 71 3C
325 Protease. *J. Med. Chem.* 58, 9414–9420.
- 326 14. Su L, Jia Y, Zhang L, Xu Y, Fang H, Xu W. 2012. Design, synthesis and biological evaluation of novel
327 amino acid ureido derivatives as aminopeptidase N/CD13 inhibitors. *Bioorg. Med. Chem.* 20, 3807–3815.
- 328 15. Galasiti Kankanamalage AC, Kim Y, Weerawarna PM, Uy RAZ, Damalanka VC, Mandadapu SR,
329 Alliston KR, Mehzabeen N, Battaile KP, Lovell S, Chang KO, Groutas WC. 2015. Structure-Guided Design
330 and Optimization of Dipeptidyl Inhibitors of Norovirus 3CL Protease. *Structure–Activity Relationships and*
331 *Biochemical, X-ray Crystallographic, Cell-Based, and In Vivo Studies. J. Med. Chem.* 58, 3144–3155.
- 332
- 333
- 334